https://doi.org/10.5194/egusphere-2026-6712
Preprint. Discussion started: 17 November 2026
© Author(s) 2026. CC BY 4.0 License.

# Eight Decades of Glacier Retreat on Heard Island: Greater Losses in More Sheltered Terrain

Richard Porter-Smith[1,2], Shavawn Donoghue[1], Sarah S. Thompson[2,3], and Benjamin K. Galton-Fenzi[1,2,3]

[1]Australian Antarctic Division, Kingston, Tasmania, Australia
[2]Australian Antarctic Program Partnership, Institute for Marine and Antarctic Studies, University of Tasmania, Australia
[3]Australian Centre for Excellence in Antarctic Science, University of Tasmania, Australia

**Correspondence:** Richard Porter-Smith (R.Smith@utas.edu.au)

**Abstract.** Over the past eight decades, Heard Island's glaciers have undergone substantial retreat, with greater fractional losses among glaciers in more sheltered terrain, contrary to a simple expectation of greater retreat in more exposed settings. Using glacier inventories spanning 1947–2025 for Big Ben and the latest available mapping from 2017 for the Laurens Peninsula, we quantify losses in glacier area and first-order estimated ice volume and examine their spatial associations with terrain exposure, glacier geometry, and regional climate variability across 28 glacier basins. Total glacierised area decreased from 283.73 to 217.96 km$^2$ (23.2 %), while first-order estimated ice volume decreased from 17.59 to 12.08 km$^3$ (31.3 %), equivalent to approximately 4.96 Gt of ice under an assumed density of 900 kg m$^{-3}$. Losses were strongly spatially heterogeneous, with particularly large fractional losses on the Laurens Peninsula and substantial retreat among several eastern and southeastern Big Ben glaciers. Glacier-median Sheltered Index (SI) was negatively correlated with signed fractional area change ($r = -0.609$, $p < 0.001$) and estimated-volume change ($r = -0.673$, $p < 0.001$), consistent with greater fractional losses among relatively sheltered, higher-SI glaciers. An attribute-based classification using SI, median elevation, and long-term area and estimated-volume change identified three quantitative response groups comprising 9, 7, and 12 glaciers, respectively. Geographic location and glacier–climate correlations were excluded from group assignment, yet the groups showed pronounced spatial organisation across Heard Island. Independently evaluated contemporaneous correlations with seasonal sea-surface temperature (SST) and wind-stress magnitude overlapped substantially among groups and did not identify discrete oceanic- or atmospheric-response regimes. The results indicate that regional climate variability provides a broadly shared climatic context within which local terrain and glacier characteristics are associated with substantial basin-to-basin differences in glacier loss. This regional-climate–local-modulation framework provides a basis for interpreting heterogeneous glacier response on Heard Island and other maritime Southern Ocean islands.

## 1 Introduction

### 1.1 Multi-Decadal Glacier Retreat

Field observations, aerial photography, satellite imagery, and successive glacier inventories show that Heard Island's glaciers have undergone widespread retreat since at least the mid-twentieth century (Allison and Keage, 1986; Kiernan and McConnell,

https://doi.org/10.5194/egusphere-2026-6712
Preprint. Discussion started: 17 November 2026
© Author(s) 2026. CC BY 4.0 License.

1999; Thost and Truffer, 2008; Tielidze et al., 2025). Previous island-wide mapping documents substantial glacier-area loss between 1947 and 2019, with pronounced differences in the magnitude of change among individual glacier basins (Tielidze et al., 2025). Comparable multi-decadal retreat has occurred across other maritime sub-Antarctic islands, including South Georgia and the Kerguelen Archipelago, where glacier change has been associated with regional atmospheric and oceanic variability together with local topographic and geometric characteristics (Donoghue, 2009; Mernild et al., 2015; Bakke et al., 2021).

Previous Heard Island inventories also reveal differences in terminus recession, fractional area loss, and the timing of retreat, including contrasts between the large glaciers descending from Big Ben and smaller peripheral and peninsula glaciers (Allison and Keage, 1986; Thost and Truffer, 2008; Tielidze et al., 2025). Some glacier margins retreated persistently throughout the observational period, whereas others changed more slowly or experienced greater losses during recent decades. Although previous work has documented changes in glacier extent and terminus position, less is known about whether spatial differences in long-term retreat are systematically associated with glacier geometry, terrain exposure, or regional ocean–atmosphere variability. Understanding these relationships is important for interpreting contrasting glacier trajectories within a broadly shared maritime climatic setting.

### 1.2 Study Area

Heard Island is a remote, steep volcanic island in the southern Indian Ocean at approximately 53° S. It rises to the 2745 m summit of Big Ben, from which glaciers extend radially towards a deeply embayed coastline. Approximately 30 glaciers occupy the island, many reaching low elevations near the coast (Fig. 1) (Kiernan and McConnell, 1999). The western and southern flanks are directly exposed to the prevailing westerly circulation, whereas glaciers on the eastern and northeastern flanks occupy the lee of high central topography (Thost and Truffer, 2008; Tielidze et al., 2025). This pronounced topographic asymmetry creates contrasting terrain settings over relatively short distances.

https://doi.org/10.5194/egusphere-2026-6712
Preprint. Discussion started: 17 November 2026
© Author(s) 2026. CC BY 4.0 License.

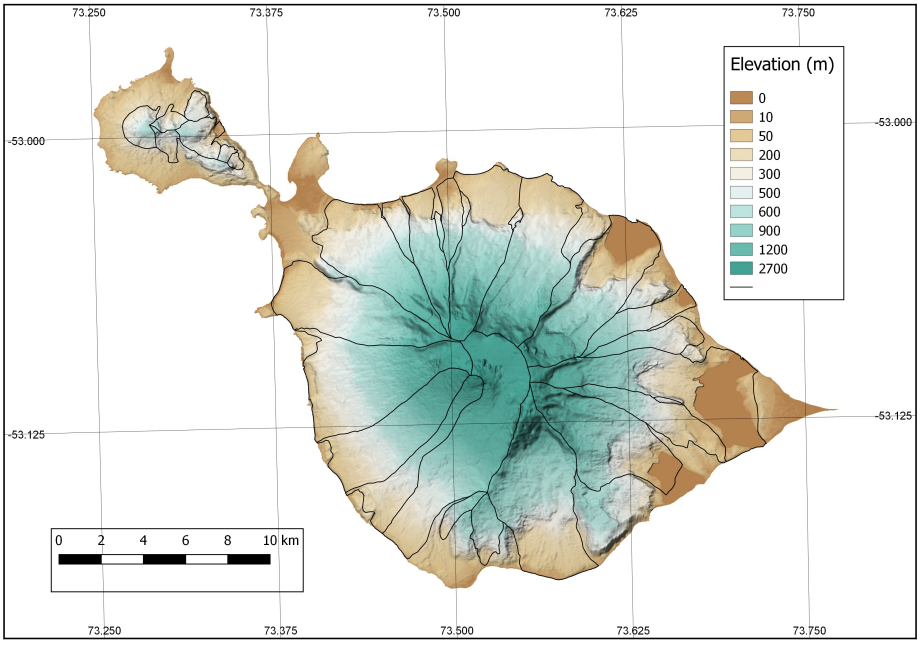



**Figure 1.** Regional location and topographic setting of Heard Island. The map shows the major glacier catchments, the summit of Big Ben, Laurens Peninsula, and glacier outlines over a hillshaded digital elevation model (2009). A $2^\circ \times 2^\circ$ ocean-reanalysis domain over the island was used to calculate spatially averaged sea-surface temperature and wind-related climate variables analysed in this study.

### 1.3 Southern Ocean Climate Context

Heard Island has a distinctly maritime glacier system characterised by persistent cloud cover, high humidity, frequent precipitation, and strong exchanges of heat and moisture between the glacier surface and atmosphere (King and Turner, 1997). Rapidly moving low-pressure systems and frontal passages produce variability in wind, cloud, temperature, and precipitation, with potential consequences for ablation and accumulation (**?**Mott et al., 2020; Nicholson and Stiperski, 2020). Across maritime sub-Antarctic islands, ocean temperature, atmospheric circulation, storm frequency, and precipitation variability influence the climatic conditions under which glacier accumulation and ablation occur (Chassiot et al., 2024; Holland, 2016; Rudolph et al., 2024; Zanker et al., 2024).

Regional ocean conditions influence lower-atmospheric temperature and moisture, while variations in the strength and position of the Southern Hemisphere westerlies affect storm tracks and the transport of heat, moisture, and precipitation (Deng et al., 2022; Perren et al., 2020; Shaw et al., 2022). The Southern Ocean has undergone changes in temperature, freshwater content, stratification, and circulation (Rintoul, 2018). Over similar timescales, the westerlies have varied in strength and latitude in association with greenhouse-gas forcing, stratospheric ozone change, and variability in the Southern Annular Mode (Marshall, 2003; Thompson et al., 2011).

https://doi.org/10.5194/egusphere-2026-6712
Preprint. Discussion started: 17 November 2026
© Author(s) 2026. CC BY 4.0 License.

Seasonal sea-surface temperature (SST) characterises aspects of the regional oceanic state and can influence the temperature and moisture of maritime air masses (Desbiolles et al., 2018; Wei and Chen, 2025). Surface wind-stress magnitude provides an indicator of regional atmospheric circulation rather than a direct measurement of turbulent heat exchange at glacier surfaces. Both variables describe elements of the regional climatic context, but neither directly measures glacier surface-energy or mass-balance conditions. Seasonal variability may be relevant to glacier change because accumulation, melt, and evolving glacier geometry can influence subsequent glacier behaviour (Cai et al., 2023; Holland et al., 2020; Oerlemans, 2001; Roe, 2010) .

### 1.4 Terrain Exposure, Glacier Geometry, and Spatially Variable Response

The expression of regional atmospheric conditions on individual glaciers may depend on terrain exposure, elevation, glacier geometry, and topographic setting. On Heard Island, precipitation amount and phase, wind-driven snow redistribution, and avalanche delivery from Big Ben's steep upper slopes may affect accumulation (Bakke et al., 2021; Clem et al., 2022; Gorodetskaya et al., 2023). Topography can also modify near-surface wind, cloud, precipitation, and surface-energy conditions (Mott et al., 2020; Shaw et al., 2024). Studies of Heard Island and other sub-Antarctic islands indicate that glacier change can differ substantially over short distances (Donoghue, 2009; Mernild et al., 2015; Bakke et al., 2021; Tielidze et al., 2025).

Local terrain and glacier geometry can influence the distribution of accumulation and ablation conditions. Elevation, hypsometry, glacier size, slope, and terminus setting are relevant to the area of ice exposed to different conditions (Allison and Keage, 1986; Kiernan and McConnell, 1999; Thost and Truffer, 2008; Brun et al., 2019; Noël et al., 2020). The effects of terrain exposure need not follow a simple exposed–sheltered gradient: greater wind exposure can modify turbulent heat exchange and snow redistribution, while sheltering may alter cloud, precipitation, and radiative conditions (Dadić et al., 2010; Evans, 1977; Mott et al., 2020). Their net influence depends on interactions among these processes and glacier geometry; their relative importance has not been quantified for individual Heard Island glacier basins.

Regional climate variability therefore provides a broadly shared climatic context within which local terrain and glacier characteristics may be associated with spatially heterogeneous glacier change. This regional-climate–local-modulation framework motivates a comparison of glacier-specific characteristics without assuming that glaciers occupying similar terrain settings necessarily share a distinct physical response mechanism.

### 1.5 Study Objectives

Building on the multi-temporal glacier inventory of Tielidze et al. (2025), the present study extends the observational record to 2025 for Big Ben using newly available glacier mapping. Persistent cloud cover prevented reliable remapping of the Laurens Peninsula after 2017, so its 2017 outlines are retained in the nominal 2019 and 2025 inventory fields. The mapped outlines used in the analysis are shown in Fig. 2. We examine spatial variability in glacier area and first-order estimated volume and their associations with terrain exposure, glacier geometry, and regional climate variability. Four questions are addressed:

https://doi.org/10.5194/egusphere-2026-6712
Preprint. Discussion started: 17 November 2026
© Author(s) 2026. CC BY 4.0 License.

1. How did glacier area and first-order estimated volume change across Heard Island from 1947 to the final mapped inventory endpoint (2025 for Big Ben and 2017 for the Laurens Peninsula), and how did the magnitude of change vary among individual glacier basins?
2. How are spatial differences in long-term glacier change associated with basin-scale terrain exposure and glacier geometry?
3. Are seasonal sea-surface temperature and wind-stress magnitude contemporaneously associated with temporal variations in glacier change?
4. Which combinations of terrain exposure, glacier geometry, and long-term change characterise glaciers with contrasting response trajectories, and how do independently evaluated seasonal climate associations vary among these groups?

The analysis combines the glacier inventory with basin-scale terrain and glacier attributes and regional seasonal climate records. An attribute-based classification summarises recurring combinations of glacier characteristics and long-term change; geographic patterns and glacier–climate associations are evaluated independently of group assignment.

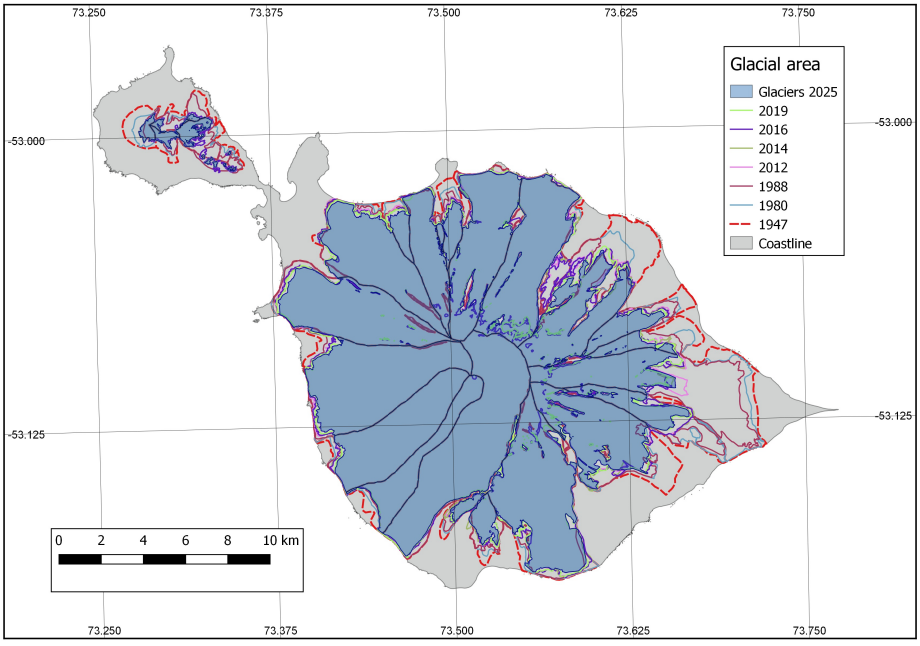



**Figure 2.** Multi-temporal glacier outlines for Heard Island from 1947 to the final inventory endpoint. The observational endpoint is 2025 for Big Ben and 2017 for the Laurens Peninsula, where persistent cloud cover prevented reliable subsequent remapping. Glacier polygons for the available inventory epochs are overlaid on a composite basemap, illustrating the spatially heterogeneous pattern of glacier retreat across Big Ben and the Laurens Peninsula. Colours represent time-ordered glacier outlines and provide the observational basis for the glacier-area analyses used in this study.

https://doi.org/10.5194/egusphere-2026-6712
Preprint. Discussion started: 17 November 2026
© Author(s) 2026. CC BY 4.0 License.

## 2 Methods

### 2.1 Overview and Analytical Framework

The methodological framework integrates multi-temporal glacier inventories, terrain and glacier morphometry, first-order ice-volume estimates, and regional climate data to quantify the magnitude and spatial variability of glacier change on Heard Island. Four complementary components were analysed:

1. Multi-temporal glacier inventories (1947, 1980, 1988, 2012, 2014, 2016, 2019, and 2025) to quantify changes in glacier area and provide the basis for first-order volume estimation.
2. DEM-derived glacier morphometry and a Sheltered Index (SI) to characterise glacier geometry and relative basin-scale terrain exposure.
3. Seasonal sea-surface temperature (SST) and surface wind-stress variables to characterise the regional oceanic and atmospheric environment surrounding Heard Island.
4. An attribute-based classification using terrain exposure, elevation, and long-term glacier loss to summarise recurring patterns of glacier response.

These components provide a consistent framework for evaluating spatially heterogeneous glacier loss within a broadly shared regional climatic setting. Regional climate variables are treated as indicators of the oceanic and atmospheric environment, rather than direct measurements of glacier-scale forcing. SI and glacier morphometry characterise local terrain and glacier attributes, while glacier–climate correlations are evaluated independently of the response-group classification.

### 2.2 Glacier Inventory Development

The glacier inventory comprises eight nominal epochs between 1947 and 2025. The early inventories were derived from aerial photography and, for the 1988 epoch, SPOT 1 satellite imagery, whereas the later inventories were derived from high-resolution satellite imagery. Source imagery, acquisition dates, spatial resolution, and processing information are summarised in Table 1. The 2025 Pléiades imagery provided updated glacier coverage for Big Ben, but persistent cloud cover prevented reliable remapping of the Laurens Peninsula. The Laurens Peninsula has not been successfully resurveyed since 2017; consequently, its most recent available glacier outlines were retained in the nominal 2025 inventory. Long-term change estimates for Laurens Peninsula therefore represent change to its most recent mapped glacier extent rather than independently observed change to 2025.

https://doi.org/10.5194/egusphere-2026-6712
Preprint. Discussion started: 17 November 2026
© Author(s) 2026. CC BY 4.0 License.

**Table 1.** Glacier inventory metadata for Heard Island (1947–2025). Summary of source imagery, spatial resolution, and acquisition information for each inventory epoch. Glacier outlines were standardised to a common coordinate system and analysis grid to maintain temporal comparability. For the Laurens Peninsula, persistent cloud cover prevented reliable remapping after 2017; the 2017 outlines were therefore retained in the nominal 2019 and 2025 inventories.

**A. Imagery and data sources**

| Date | Source imagery / dataset | Resolution | Notes |
|---|---|---|---|
| Dec 1947 | Aerial photography | – | First aerial photographic coverage; camera unknown. |
| Mar 1980 | Hasselblad aerial photography | – | Coastal imagery acquired using a Hasselblad camera. |
| 18–19 Oct 1987 / 4 Jan 1988 | Aerial photography / SPOT 1 | 10 m (SPOT 1) | Non-metric Hasselblad and Linhof photography supplemented by SPOT 1 imagery. |
| 2 Feb 2012 | GeoEye-1 | 1.84 m | First near-cloud-free image acquired on a single day. |
| 6 Feb 2014 | GeoEye-1 | 1.84 m | – |
| 21 Feb 2016 | WorldView-2 | 1.84 m | – |
| 2 Mar 2017 | WorldView-3 | 0.31 m | note - LP only |
| 13 Jan / 10 Mar 2019 | WorldView-3 | 0.31 m | Big Ben inventory; Laurens Peninsula retained from 2017. |
| Apr 2025 | Pléiades | 0.5 m | Big Ben inventory; Laurens Peninsula retained from 2017. |

**B. Processing consistency across epochs**

| Processing component | Method | Notes |
|---|---|---|
| Projection | UTM Zone 43S | Standardised across all years. |
| Rasterisation | 10 m grid | Common grid for area and terrain analyses. |
| Manual editing | Cloud, shadow, and debris handling | Consistent interpretation criteria across epochs. |
| Topological checks | Polygon validity and sliver removal | Ensures compatibility with DEM-based analyses. |

All glacier boundaries were reviewed using consistent interpretation criteria. The mapped boundary followed the visible transition between glacier ice or snow and adjacent exposed terrain. Seasonal snow outside the persistent glacier margin was excluded where it could be distinguished from glacier ice. Debris-covered ice was retained where surface texture, flow structures, continuity with exposed ice, or comparison with adjacent epochs supported its interpretation as glacier ice. Sections obscured by cloud or shadow were checked against neighbouring imagery and adjacent inventory epochs rather than inferred from image tone alone.

https://doi.org/10.5194/egusphere-2026-6712
Preprint. Discussion started: 17 November 2026
© Author(s) 2026. CC BY 4.0 License.

Persistent cloud cover prevented reliable remapping of the Laurens Peninsula after 2017. Consequently, the 2017 Laurens Peninsula outlines were retained in the nominal 2019 and 2025 inventory fields, whereas the 2025 inventory provides an updated observational endpoint for Big Ben. Long-term changes reported for the Laurens Peninsula therefore extend from 1947 to its most recent mapped glacier extent in 2017, rather than to an independently observed 2025 extent.

Following review, all outlines were transformed to UTM Zone 43S and rasterised to a common 10 m analysis grid for area, terrain, and zonal-statistics calculations. Polygon geometry was checked for topological errors, and isolated polygons, narrow slivers, and mapping artefacts unsupported by the source imagery were removed. Glacier identifiers and drainage-basin assignments were maintained consistently among inventory epochs.

### 2.3 Digital Elevation Model and Terrain Metrics

A TerraSAR-X digital elevation model acquired in 2009 was used to derive glacier elevation, surface slope, aspect, and hypsometric variables. The 2009 DEM was applied as a fixed reference surface throughout the analysis. For the first-order thickness calculations, the corresponding slope field was intersected with the glacier outline from each inventory epoch. Temporal differences in estimated volume therefore reflect changes in mapped glacier extent evaluated using a fixed reference geometry and do not reconstruct changes in glacier surface elevation or slope through time.

Available elevation datasets were examined for independent DEM differencing, but differences in acquisition geometry, radar penetration, spatial coverage, geolocation, and data completeness prevented a robust island-wide geodetic comparison. The slope-based estimates are therefore not interpreted as observed elevation or volume change. Instead, they provide first-order comparative estimates of glacier volume under a consistent geometric approximation.

Terrain exposure was quantified using a DEM-derived Sheltered Index (SI) designed to represent relative topographic sheltering with respect to the prevailing wind environment. The directional exposure metric was calculated as

$$E_{\text{weighted}} = \frac{\sum_i w_i[-\cos(\text{aspect} - \theta_i)\sin(\text{slope})]}{\sum_i w_i}, \tag{1}$$

where $i$ denotes the wind samples, $\theta_i$ is wind direction, and $w_i$ is wind-stress magnitude. The resulting exposure values were normalised to SI values ranging from 0 (relatively exposed) to 1 (relatively sheltered) (McCune and Keon, 2002; Ryan, 1977).

For each glacier, SI was extracted within the glacier polygon and summarised using the median of all valid raster cells. The median reduces sensitivity to isolated extreme values near steep ridges and glacier boundaries. Seasonal SI values were calculated for DJF, MAM, JJA, and SON, and their median was used to provide a single glacier-scale measure of relative terrain exposure. SI therefore represents relative basin-scale topographic sheltering with respect to the wind environment and does not directly quantify local wind speed, turbulent heat exchange, cloud conditions, or precipitation.

### 2.4 First-order Glacier Thickness and Volume Estimation

Ice thickness was approximated using a slope-dependent relationship (Cuffey and Paterson, 2010; Farinotti et al., 2009):

https://doi.org/10.5194/egusphere-2026-6712
Preprint. Discussion started: 17 November 2026
© Author(s) 2026. CC BY 4.0 License.

$$H = \frac{\tau}{\rho g \sin \alpha}, \tag{2}$$

where $H$ is estimated ice thickness, $\tau$ is the assumed basal shear stress, $\rho$ is ice density, $g$ is gravitational acceleration, and $\alpha$ is glacier surface slope. In this formulation, glacier driving stress is approximated from surface slope and a spatially uniform basal shear stress. We used $\tau = 100 \pm 25$ kPa, $\rho = 900\,\mathrm{kg\,m^{-3}}$, and $g = 9.81\,\mathrm{m\,s^{-2}}$, consistent with first-order approximations for mountain and valley glaciers (Cuffey and Paterson, 2010; Farinotti et al., 2009). These parameters were not calibrated using ice-thickness observations from Heard Island, and the resulting estimates are therefore used for comparative rather than geodetic purposes.

For each glacier and inventory epoch, estimated ice thickness was integrated over the mapped glacier area to obtain a first-order volume estimate. The relationship between mapped glacier area and these estimated volumes was subsequently represented using an empirical power law,

$$V = cA^{\gamma}, \tag{3}$$

where $V$ is estimated glacier volume ($\mathrm{km^3}$), $A$ is glacier area ($\mathrm{km^2}$), $c$ is a fitted coefficient, and $\gamma$ is the fitted area–volume exponent. The functional form follows the general area–volume scaling approach of Bahr et al. (1997), but published scaling coefficients were not prescribed. Instead, $c$ and $\gamma$ were fitted separately for each glacier using the available area and first-order volume estimates from the eight inventory epochs.

The power law was fitted by ordinary least-squares regression in logarithmic space,

$$\ln(V) = \ln(c) + \gamma \ln(A), \tag{4}$$

with $\gamma$ obtained from the regression slope and $c$ from the exponentiated intercept. The coefficient of determination ($R^2$) was calculated in log–log space to describe the internal fit between glacier area and the corresponding first-order volume estimates. Because these same volume estimates were used to calibrate the glacier-specific relationships, the area–volume scaling is not an independent validation of glacier thickness or volume. It provides an interpolation framework for generating internally consistent estimated volumes from the glacier-area trajectories.

For comparison between the irregularly spaced glacier inventories and the climate record, glacier area was interpolated to regular five-year intervals using piecewise cubic Hermite interpolation (PCHIP). PCHIP was selected because it preserves the shape of the observed area trajectory between successive inventory epochs without imposing oscillations associated with higher-order spline interpolation (Fritsch and Carlson, 1980).

At each interpolated time step, estimated glacier volume was calculated from the glacier-specific area–volume relationship,

$$V_t = cA_t^{\gamma}, \tag{5}$$

https://doi.org/10.5194/egusphere-2026-6712
Preprint. Discussion started: 17 November 2026
© Author(s) 2026. CC BY 4.0 License.

rather than by direct interpolation between discrete volume estimates. The original first-order volume estimates therefore constrain the fitted scaling relationship, while temporal variation within each inventory interval is determined by the interpolated glacier-area trajectory.

For climate comparison, changes in estimated volume between successive five-year time steps were converted to mean estimated mass-loss rates using a constant ice density of 900 kg m$^{-3}$. Because mass is derived directly from estimated volume using a fixed density, mass is not treated as an independent measure of glacier change.

The interpolated area, estimated-volume, and derived mass-loss values are not independent glacier observations and are not used to infer short-term glacier dynamics or annual mass balance. They provide temporally consistent trajectories for comparison with the regional climate record.

### 2.5 Regional Climate Data

Regional oceanic and atmospheric conditions were characterised using monthly sea-surface temperature (SST) and surface wind-stress fields from the European Centre for Medium-Range Weather Forecasts (ECMWF) Ocean Reanalysis System 5 (ORAS5; backward-extension product). The fields were provided on the native, non-uniform ORAS5 ocean grid, with geographic coordinates specified by the two-dimensional `nav_lon` and `nav_lat` variables. SST was obtained from `sosstsst` (°C), and the zonal and meridional surface wind-stress components from `sozotaux` and `sometauy`, respectively (N m$^{-2}$).

Surface wind-stress magnitude was calculated from the horizontal stress components as

$$\tau_{\mathrm{w}} = \sqrt{\tau_x^2 + \tau_y^2}, \tag{6}$$

where $\tau_{\mathrm{w}}$ denotes wind-stress magnitude and $\tau_x$ and $\tau_y$ denote the zonal and meridional surface wind-stress components, respectively. Wind direction and the fraction of winds originating from the westerly sector were also derived from the horizontal components. Westerly fraction was defined as the proportion of vectors within the 225–315° directional sector (Sallée et al., 2021; Thompson et al., 2011).

Monthly SST and wind-stress values were spatially averaged across the 2° × 2° domain surrounding Heard Island shown in Fig. 1 and aggregated into austral summer (DJF), autumn (MAM), winter (JJA), and spring (SON) means. Seasonal climate data were extracted for 1965–2025.

SST and wind-stress variables were treated as regional indicators of the oceanic and atmospheric environment surrounding Heard Island rather than direct measurements of glacier-scale surface-energy fluxes.

### 2.6 Glacier–Climate Comparison

Seasonal climate variables were compared with five-year glacier-change trajectories to evaluate contemporaneous associations between glacier change and regional oceanic and atmospheric variability. The climate dataset comprised seasonal SST, wind-stress magnitude, wind direction, and westerly fraction for DJF, MAM, JJA, and SON. Climate values were matched by calendar year to the corresponding five-year glacier series.

https://doi.org/10.5194/egusphere-2026-6712
Preprint. Discussion started: 17 November 2026
© Author(s) 2026. CC BY 4.0 License.

The climate data represent a single regional time series for Heard Island. Each glacier was therefore compared with the same seasonal climate values at each time step. Differences among glacier–climate correlations consequently reflect differences among the glacier-change trajectories rather than spatial differences in the prescribed climate data.

For each glacier, Pearson correlation coefficients were calculated between the glacier-change series and each seasonal climate variable using only time steps for which both values were finite, with a minimum of three paired values required. The resulting coefficients describe the direction and strength of contemporaneous linear associations. Glacier and climate values with the same five-year time stamp were compared directly; no temporal lags were introduced.

Because the five-year glacier trajectories are interpolated between a limited number of independent inventory epochs, successive values are not equivalent to independent annual observations of glacier mass balance. The correlations are therefore interpreted as exploratory, descriptive measures rather than formal tests of climatic control. SST and wind-stress correlations were not used to assign the attribute-based response groups described in Sect. 2.7, allowing climate associations to be compared independently among the resulting groups.

### 2.7 Attribute-based Classification of Glacier Response

To summarise recurring combinations of terrain setting, glacier geometry, and long-term glacier loss, the 28 glacier basins were assigned to three comparative response groups (A–C) using a transparent rule-based classification. The classification was designed as a descriptive framework for comparing glacier responses rather than as an identification of discrete physical glacier types.

Three components were used in the classification: basin-scale terrain exposure represented by SI, glacier elevation, and observed long-term glacier loss. Glacier-median SI was calculated as the median of the DJF, MAM, JJA, and SON 2025 SI values for each basin. Glaciers were ranked by SI and divided into three approximately equal rank-based classes representing relatively exposed, intermediate, and relatively sheltered terrain settings. The lowest-SI class contributed two points to Group A, whereas the intermediate- and highest-SI classes each contributed two points to Group B. SI therefore provides the principal terrain-exposure distinction between Groups A and B.

Median glacier elevation was calculated from the fixed reference DEM within the 2025 glacier extent and included as a descriptor of glacier geometric setting. Glaciers with median elevations $\geq 650$ m received one additional Group-A point, whereas glaciers with median elevations $\leq 450$ m received two Group-C points. Long-term glacier loss represented the realised response between 1947 and 2025. Glaciers for which either absolute fractional area loss or first-order estimated-volume loss was $\geq 60\,\%$ received three Group-C points. The resulting scores were

$$S_A = 2I_{\mathrm{low\,SI}} + I_{z\geq 650}, \tag{7}$$

$$S_B = 2I_{\mathrm{middle\,SI}} + 2I_{\mathrm{high\,SI}}, \tag{8}$$

https://doi.org/10.5194/egusphere-2026-6712
Preprint. Discussion started: 17 November 2026
© Author(s) 2026. CC BY 4.0 License.

and

$$S_C = 2I_{z\leq 450} + 3I_{(|\Delta A|\geq 60\% \vee |\Delta V|\geq 60\%)}, \tag{9}$$

where $I$ denotes an indicator function, $z$ is median glacier elevation, $\Delta A$ is signed fractional area change, and $\Delta V$ is signed fractional first-order estimated-volume change. Each glacier was assigned to the group with the highest score. The final classification produced a unique highest score for all 28 glaciers.

Geographic region and longitude were excluded from the classification so that the spatial organisation of the resulting groups could be evaluated independently. Seasonal SST and wind-stress correlations were also excluded from group assignment. This separation avoids using the same climate correlations both to construct and compare the response groups, and avoids duplicating wind-related information already represented in the terrain-exposure metric. Glacier–climate correlations were instead retained as independent descriptive measures for comparison among the resulting groups.

For transparency, the three rule scores were transformed using a softmax function,

$$W_g = \frac{\exp(S_g)}{\sum_{j=A}^{C} \exp(S_j)}, \tag{10}$$

where $S_g$ is the score for group $g$. These values are reported as relative score weights only and are not statistical probabilities of group membership. Glacier-level attributes, scores, relative score weights, and final assignments are reported in Table S1.

## 3 Results

Regional climate variability is presented first to establish the environmental context shared by the Heard Island glaciers. We then quantify island-wide and glacier-specific changes in area and first-order estimated volume before examining their spatial associations with glacier geometry, hypsometry, terrain exposure, and seasonal climate variability. Finally, these attributes are synthesised using the attribute-based glacier-response classification described in Sect. 2.7.

### 3.1 Regional climate variability and trends

Seasonal climate conditions varied substantially over the regional domain surrounding Heard Island between 1965 and 2025 (Fig. 3). Sea-surface temperature (SST) increased in all four seasons over the analysis period, although the magnitude and statistical significance of the trends differed seasonally. The strongest warming occurred during JJA, at 0.12 °C decade$^{-1}$ ($p = 0.034$). Smaller positive trends occurred during MAM (0.08 °C decade$^{-1}$, $p = 0.101$), SON (0.05 °C decade$^{-1}$, $p = 0.119$), and DJF (0.02 °C decade$^{-1}$, $p = 0.783$). JJA was therefore the only season with a statistically significant linear SST trend at the 0.05 level (Table 2).

Seasonal wind-stress magnitude also showed positive linear trends in all four seasons, but none was statistically significant at the 0.05 level. The largest increase occurred during JJA (0.014 N m$^{-2}$ decade$^{-1}$, $p = 0.081$), followed by MAM (0.009 N m$^{-2}$ decade$^{-1}$,

https://doi.org/10.5194/egusphere-2026-6712
Preprint. Discussion started: 17 November 2026
© Author(s) 2026. CC BY 4.0 License.

$p = 0.153$), SON ($0.007\,\mathrm{N\,m^{-2}\,decade^{-1}}$, $p = 0.183$), and DJF ($0.003\,\mathrm{N\,m^{-2}\,decade^{-1}}$, $p = 0.574$). These records therefore indicate multi-decadal variability in the regional oceanic and atmospheric environment, with significant linear warming confined to winter SST in the present analysis.

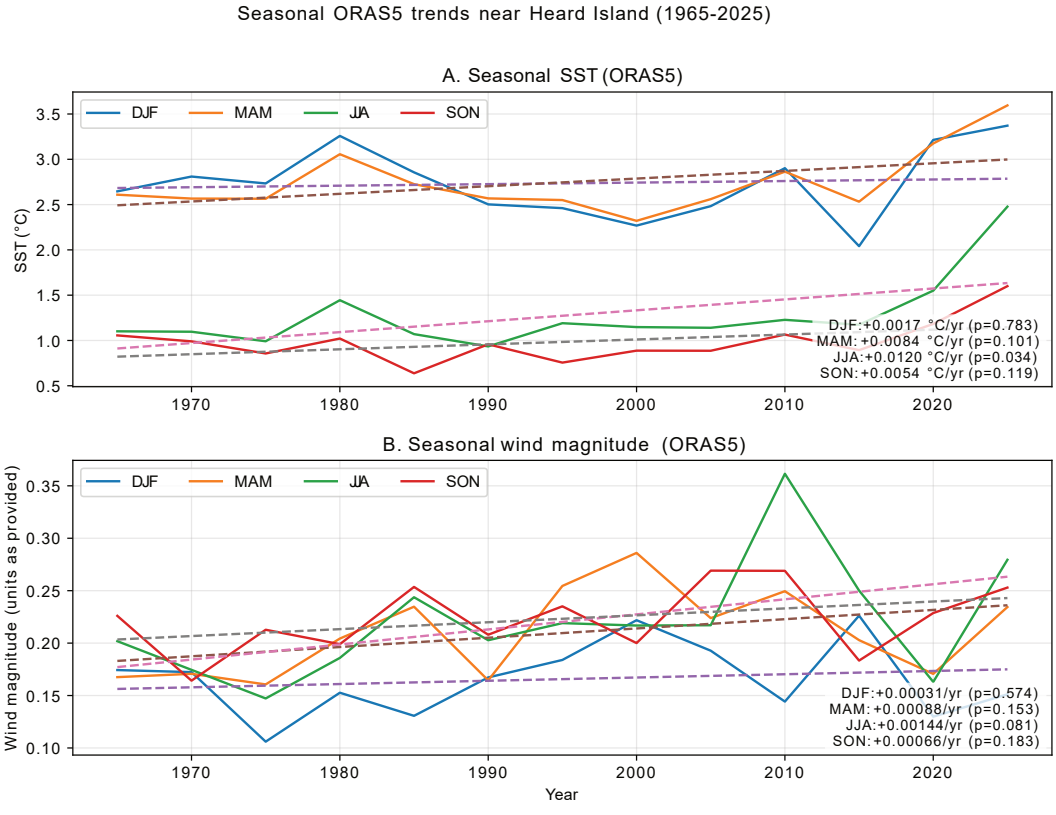



**Figure 3.** Seasonal sea-surface temperature (SST) and wind-stress magnitude ($\mathrm{N\,m^{-2}}$) variability for the $2^\circ \times 2^\circ$ region centred on Heard Island between 1965 and 2025. Lines show seasonal values for DJF, MAM, JJA, and SON, with corresponding linear trends and trend statistics. Seasonal trend magnitudes expressed per decade are summarised in Table 2.

https://doi.org/10.5194/egusphere-2026-6712
Preprint. Discussion started: 17 November 2026
© Author(s) 2026. CC BY 4.0 License.

**Table 2.** Seasonal SST and wind-stress magnitude trends for the $2^\circ \times 2^\circ$ region centred on Heard Island between 1965 and 2025.

**A. SST trends**

| Season | Trend (°C decade$^{-1}$) | $p$-value |
|---|---|---|
| DJF | 0.017 | 0.783 |
| MAM | 0.084 | 0.101 |
| JJA | 0.120 | 0.034 |
| SON | 0.054 | 0.119 |

**B. Wind-stress magnitude trends**

| Season | Trend (N m$^{-2}$ decade$^{-1}$) | $p$-value |
|---|---|---|
| DJF | 0.003 | 0.574 |
| MAM | 0.009 | 0.153 |
| JJA | 0.014 | 0.081 |
| SON | 0.007 | 0.183 |

### 3.2 Island-wide glacier area loss

Glacier area decreased substantially across Heard Island between 1947 and the nominal 2025 inventory (Fig. 2). Across the 28 glaciers included in the analysis, total glacierised area decreased from 283.73 km$^2$ in 1947 to 217.96 km$^2$ in the final inventory. This represents a net reduction of 65.77 km$^2$, equivalent to 23.18 % of the 1947 glacier area. The 2025 inventory provides an updated observational endpoint for Big Ben, whereas the most recent mapped glacier extents on the Laurens Peninsula are from 2017 and were retained in the nominal 2019 and 2025 inventory fields (Sect. 2.2).

The absolute loss was dominated by glaciers draining Big Ben. Their combined area decreased from 277.93 km$^2$ in 1947 to 216.60 km$^2$ in 2025, corresponding to a reduction of 61.33 km$^2$ (22.07 %). On the Laurens Peninsula, glacier area decreased from 5.80 km$^2$ in 1947 to 1.36 km$^2$ by the most recent mapped extent in 2017, an absolute reduction of 4.44 km$^2$ and a substantially greater fractional loss of 76.55 %.

Long-term area change varied markedly among individual glacier basins. Several eastern and southeastern Big Ben glaciers experienced substantial reductions, whereas changes were smaller for many western Big Ben glaciers. Laurens Peninsula glaciers experienced some of the largest fractional area reductions relative to their 1947 extents. Regional area and first-order estimated-volume changes are summarised in Table 3.

https://doi.org/10.5194/egusphere-2026-6712
Preprint. Discussion started: 17 November 2026
© Author(s) 2026. CC BY 4.0 License.

**Table 3.** Regional glacier area, first-order estimated-volume change, and density-equivalent mass loss from 1947 to the final inventory endpoint. The endpoint is 2025 for Big Ben and 2017 for the Laurens Peninsula, where persistent cloud cover prevented subsequent reliable remapping. The island-wide nominal 2025 inventory therefore combines 2025 Big Ben geometry with the most recent available Laurens Peninsula geometry from 2017. Estimated mass loss was calculated using an assumed ice density of 900 kg m$^{-3}$ and is not an independent mass-balance measurement. Negative percentage changes represent glacier loss.

| Region | Area 1947 (km$^2$) | Area endpoint (km$^2$) | Area change (%) | Est. volume 1947 (km$^3$) | Est. volume 2025 (km$^3$) | Est. volume change (%) | Est. mass loss (Gt) |
|---|---|---|---|---|---|---|---|
| Big Ben | 277.93 | 216.60 | −22.07 | 17.405 | 12.037 | −30.84 | 4.831 |
| Laurens Peninsula | 5.80 | 1.36 | −76.55 | 0.1844 | 0.0415 | −77.49 | 0.129 |
| Heard Island total | 283.73 | 217.96 | −23.18 | 17.590 | 12.078 | −31.33 | 4.960 |

### 3.3 Estimated glacier volume loss

First-order estimated glacier volume decreased substantially between 1947 and the final inventory endpoint. Island-wide estimated volume decreased from 17.590 km$^3$ to 12.078 km$^3$, corresponding to a reduction of approximately 5.511 km$^3$ (31.33 %). At an assumed ice density of 900 kg m$^{-3}$, this estimated-volume reduction corresponds to a density-equivalent mass loss of approximately 4.960 Gt, from 15.831 to 10.871 Gt. The proportional reduction in estimated volume was larger than the observed proportional reduction in glacier area (23.18 %).

Estimated volume for Big Ben glaciers decreased from 17.405 km$^3$ in 1947 to 12.037 km$^3$ in 2025, a reduction of approximately 5.368 km$^3$ (30.84 %), equivalent to approximately 4.831 Gt. On the Laurens Peninsula, estimated glacier volume decreased from 0.1844 km$^3$ in 1947 to 0.0415 km$^3$ by the most recent mapped extent in 2017, corresponding to a reduction of approximately 0.1429 km$^3$ (77.49 %), equivalent to approximately 0.129 Gt. The Laurens Peninsula therefore contributed little to the island-wide absolute estimated-volume reduction but experienced substantially larger fractional change.

Glacier-specific changes showed a corresponding contrast between absolute and fractional estimated-volume loss (Fig. 4). Several large Big Ben outlet glaciers accounted for substantial absolute estimated-volume reductions, whereas smaller glaciers, including those on the Laurens Peninsula, experienced some of the largest fractional reductions.

https://doi.org/10.5194/egusphere-2026-6712
Preprint. Discussion started: 17 November 2026
© Author(s) 2026. CC BY 4.0 License.

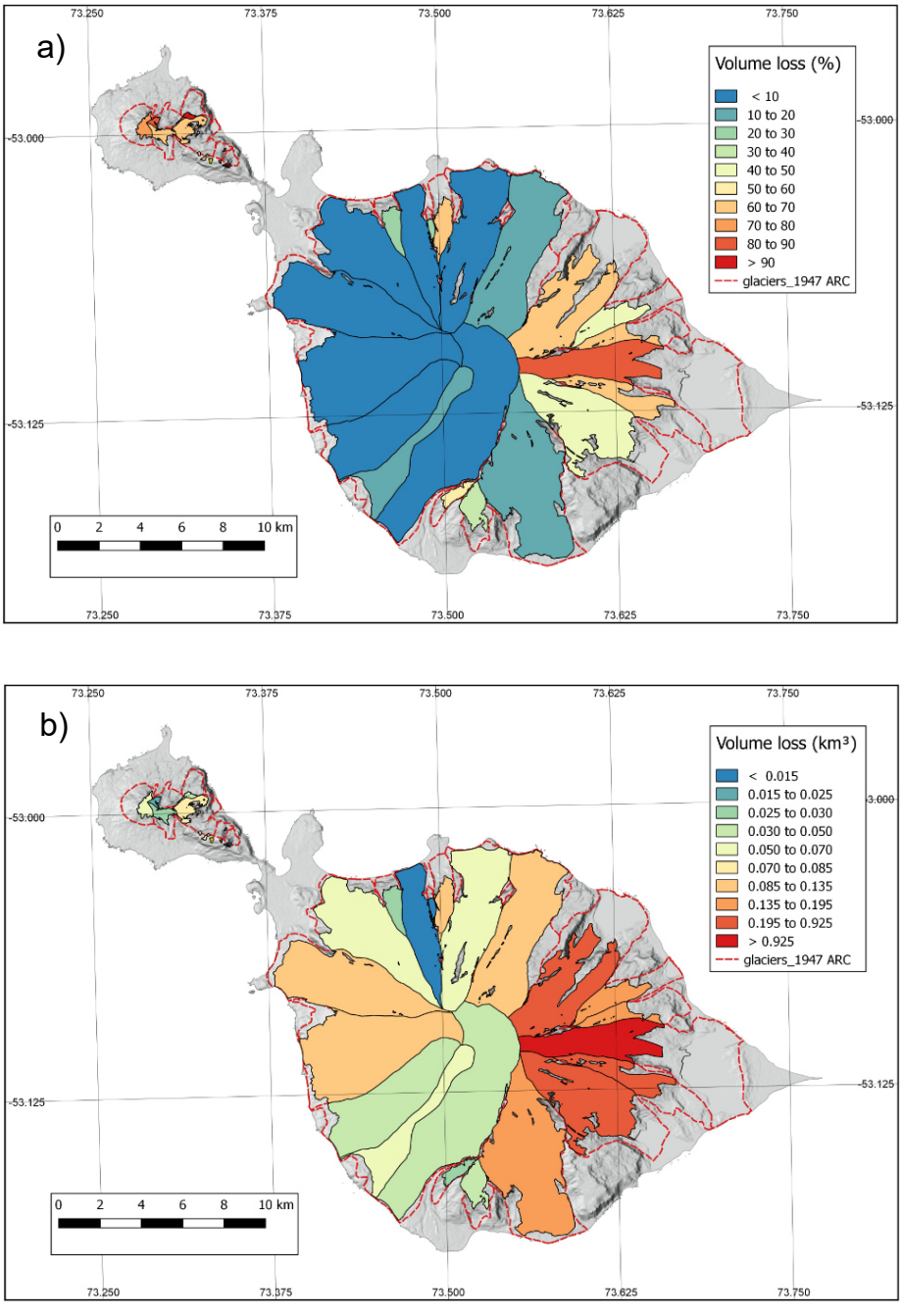



**Figure 4.** Spatial distribution of first-order estimated glacier-volume change across Heard Island from 1947 to the final inventory endpoint. (a) Fractional estimated-volume change (%) for individual glacier basins relative to estimated 1947 volume. (b) Absolute estimated-volume change ($km^3$) over the same period. The endpoint is 2025 for Big Ben and 2017 for the Laurens Peninsula. Negative values indicate estimated glacier-volume loss. Volume changes are derived from the slope-based thickness approximation and glacier-specific area–volume relationships described in Sect. 2.4 and are not direct geodetic measurements.

https://doi.org/10.5194/egusphere-2026-6712
Preprint. Discussion started: 17 November 2026
© Author(s) 2026. CC BY 4.0 License.

### 3.4 Glacier geometry and hypsometry

Glacier geometry varied substantially across Heard Island (Fig. 5; Table 4). Glaciers on Big Ben generally occupied broader and higher elevation ranges than those on the Laurens Peninsula. Median glacier elevation was 557 m for western Big Ben and 717 m for eastern Big Ben, compared with 437 m for the Laurens Peninsula. Laurens Peninsula glaciers were also substantially steeper, with a median slope of $24^\circ$, compared with $14^\circ$ and $13^\circ$ for western and eastern Big Ben, respectively.

Hypsometric distributions showed a corresponding regional contrast. Big Ben glaciers generally contained larger areas at higher elevations and broader elevation ranges, whereas Laurens Peninsula glaciers had more restricted high-elevation areas. These geometric differences occurred alongside marked differences in long-term glacier loss. Median fractional area change was $-10.77\,\%$ for western Big Ben, $-42.39\,\%$ for eastern Big Ben, and $-81.42\,\%$ for the Laurens Peninsula. Corresponding median first-order estimated-volume changes were $-12.50\,\%$, $-47.28\,\%$, and $-78.87\,\%$, respectively.

https://doi.org/10.5194/egusphere-2026-6712
Preprint. Discussion started: 17 November 2026
© Author(s) 2026. CC BY 4.0 License.

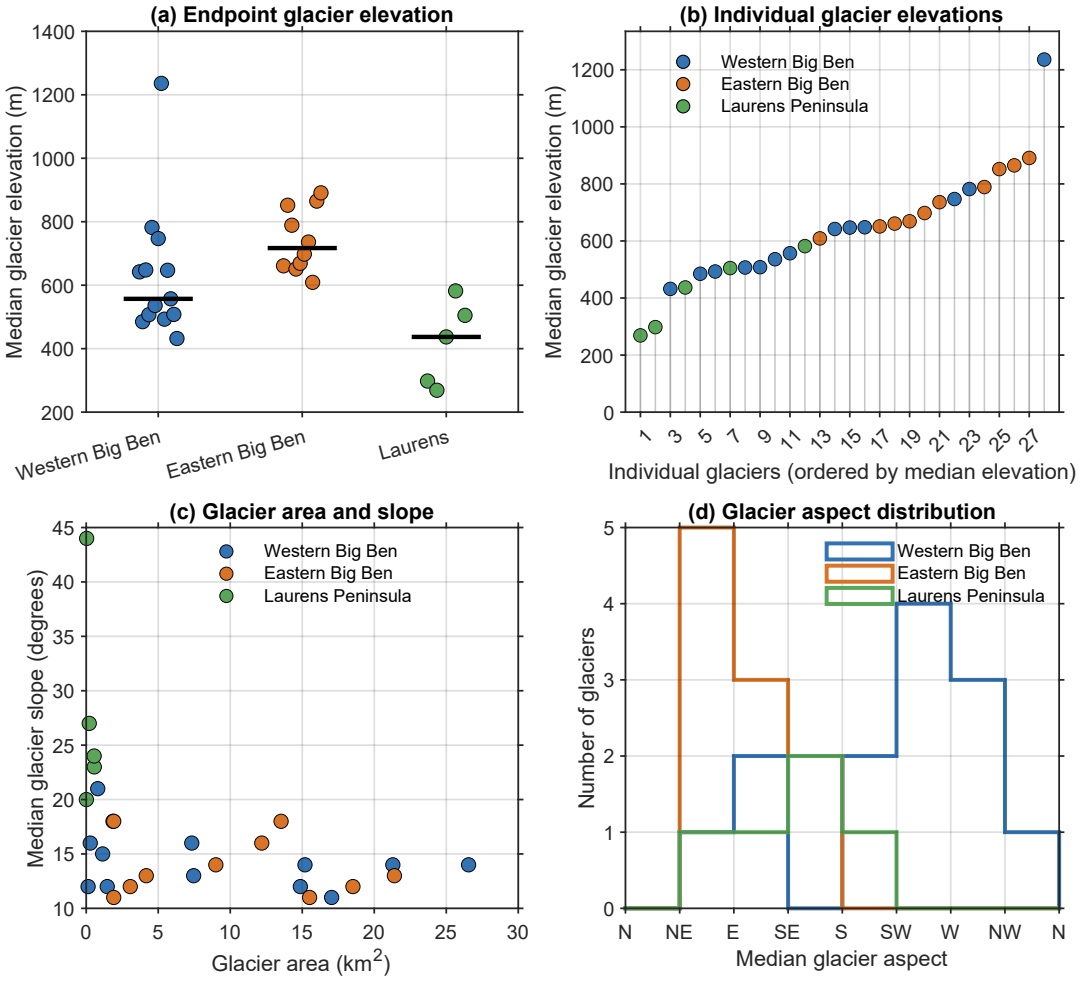



**Figure 5.** Glacier morphology and elevation characteristics across Heard Island. (a) Distribution of glacier-median elevation among western Big Ben, eastern Big Ben, and Laurens Peninsula glaciers; horizontal bars indicate sector medians. (b) Individual glacier-median elevations ordered from lowest to highest and coloured by geographic sector. (c) Relationship between glacier area and median glacier slope. (d) Distribution of glacier-median aspect. Glacier geometry corresponds to the 2025 extent for Big Ben and the most recent mapped extent (2017) for the Laurens Peninsula.

320 Median glacier slope was negatively correlated with signed fractional area change ($r = -0.568$, $p = 0.0016$, $n = 28$), with steeper glaciers tending to show more negative fractional area changes. The change interval extends from 1947 to 2025 for Big Ben and from 1947 to the most recent mapped extent in 2017 for the Laurens Peninsula. Spatial variations in glacier slope and aspect are shown in Fig. 6.

https://doi.org/10.5194/egusphere-2026-6712
Preprint. Discussion started: 17 November 2026
© Author(s) 2026. CC BY 4.0 License.

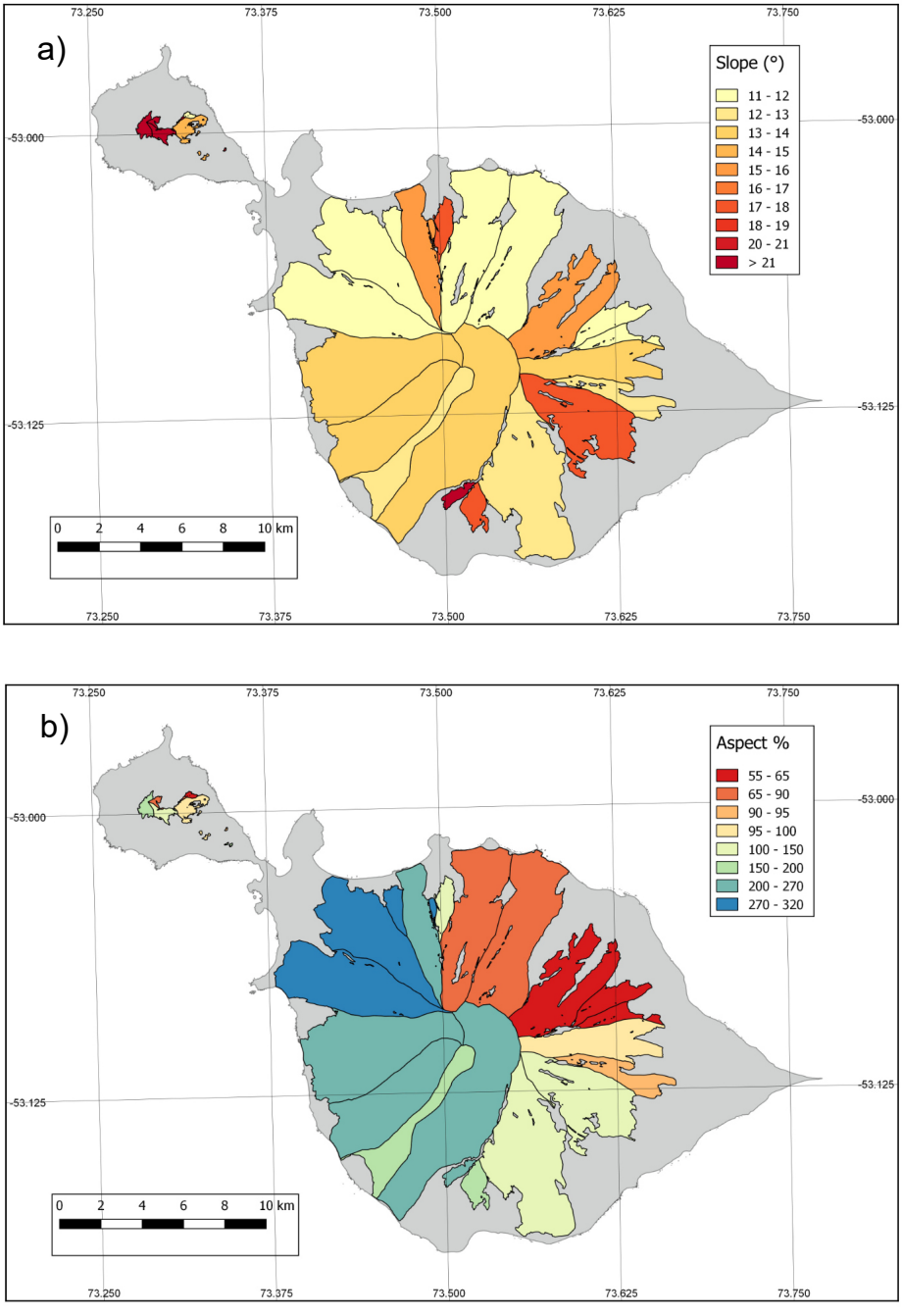



**Figure 6.** Glacier slope and aspect across Heard Island. (a) Glacier surface slope and (b) surface aspect derived from the fixed reference DEM.

https://doi.org/10.5194/egusphere-2026-6712
Preprint. Discussion started: 17 November 2026
© Author(s) 2026. CC BY 4.0 License.

No statistically significant relationship was detected between glacier aspect and long-term glacier loss. Terrain exposure also differed among the geographic sectors. Median SI increased from 0.447 for western Big Ben to 0.559 for eastern Big Ben and 0.592 for the Laurens Peninsula (Table 4). The sectors with higher median SI therefore also exhibited greater median fractional glacier loss, although substantial variability between glaciers remained. The glacier-scale relationship between SI and long-term change is examined directly in Sect. 3.5.

**Table 4.** Glacier morphometry, terrain exposure, and long-term change summarised by geographic sector. Values are medians, with glacier-median SI ranges shown in parentheses. Negative area and estimated-volume changes represent glacier loss. Change intervals extend from 1947 to 2025 for Big Ben and from 1947 to the most recent mapped extent in 2017 for the Laurens Peninsula.

| Region | $n$ | Median SI (range) | Elevation (m) | Slope (°) | Area change (%) | Est. volume change (%) |
|---|---|---|---|---|---|---|
| Western Big Ben | 13 | 0.447 (0.349–0.554) | 557 | 14 | −10.77 | −12.50 |
| Eastern Big Ben | 10 | 0.559 (0.509–0.615) | 717 | 13 | −42.39 | −47.28 |
| Laurens Peninsula | 5 | 0.592 (0.489–0.649) | 437 | 24 | −81.42 | −78.87 |

### 3.5 Basin-scale terrain exposure

The Sheltered Index (SI) showed substantial spatial variability in terrain exposure across Heard Island that was not represented by a simple windward–leeward division (Fig. 7). Lower SI values indicate greater relative exposure to the prevailing wind environment, whereas higher values indicate greater terrain sheltering. Glacier-scale median SI values nevertheless integrate substantial within-basin variation in topographic exposure.

https://doi.org/10.5194/egusphere-2026-6712
Preprint. Discussion started: 17 November 2026
© Author(s) 2026. CC BY 4.0 License.

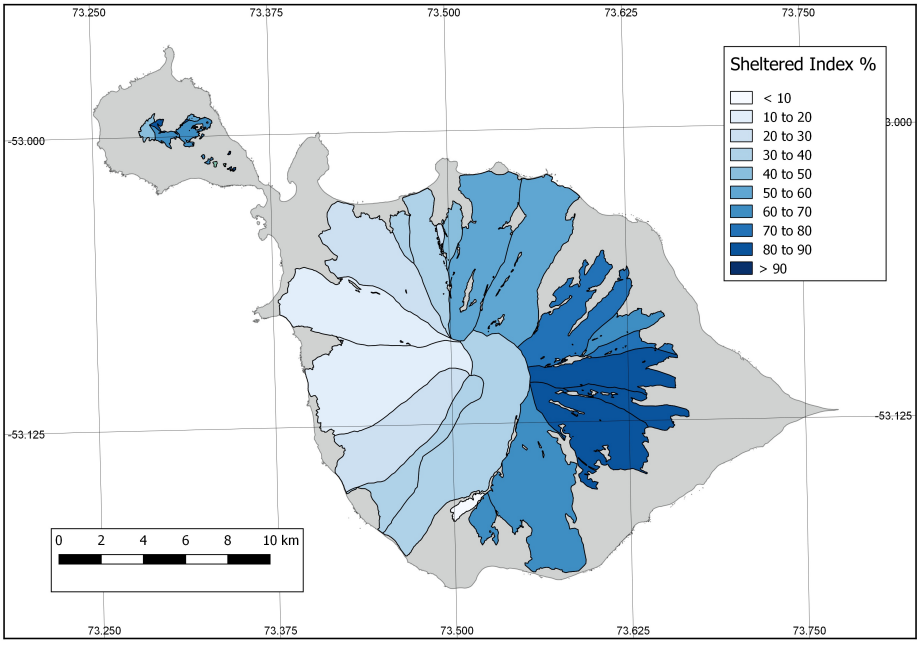



**Figure 7.** Spatial distribution of the DEM-derived Sheltered Index (SI) across Heard Island. Lower SI values indicate greater relative terrain exposure and higher values indicate greater sheltering. Glacier polygons are classified using glacier-median SI, illustrating broad contrasts in terrain exposure among individual basins while retaining substantial within-glacier variability.

For comparative analysis, glaciers were divided into three approximately equal rank-based classes according to glacier-median SI. The lowest-SI class represents the most exposed glacier basins, the middle class represents intermediate conditions, and the highest-SI class represents the most sheltered basins. These classes describe relative exposure within the Heard Island glacier population rather than fixed physical thresholds.

Glacier-median SI was significantly correlated with both fractional area change and first-order estimated-volume change (Fig. 8). Fractional area change was negatively correlated with SI ($r = -0.609$, $p = 0.00059$, $n = 28$; $r^2 = 0.37$), as was estimated-volume change ($r = -0.673$, $p = 8.7 \times 10^{-5}$, $n = 28$; $r^2 = 0.45$). The change interval extends from 1947 to 2025 for Big Ben and from 1947 to the most recent mapped extent in 2017 for the Laurens Peninsula. Because glacier change is expressed as a signed percentage, with negative values representing loss, these relationships indicate that glaciers with higher SI values generally experienced larger long-term fractional area and estimated-volume loss. Several high-SI glaciers with large fractional losses occur on eastern and southeastern Heard Island.

https://doi.org/10.5194/egusphere-2026-6712
Preprint. Discussion started: 17 November 2026
© Author(s) 2026. CC BY 4.0 License.

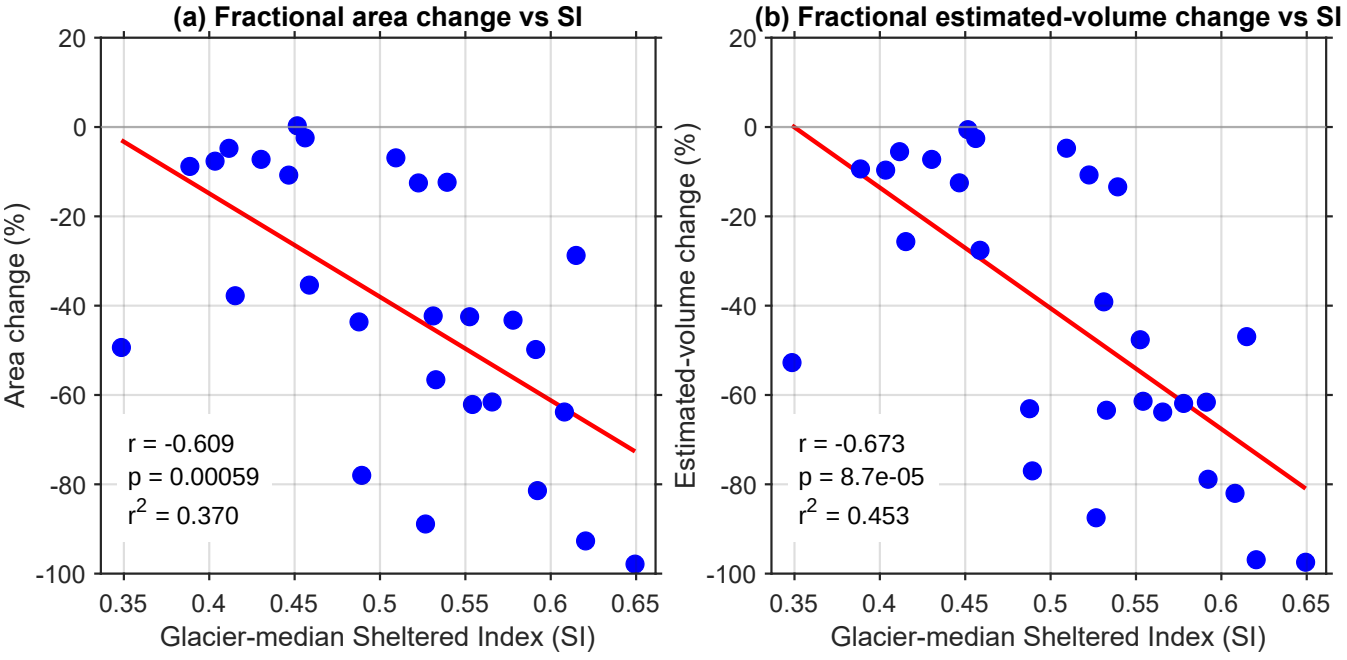



**Figure 8.** Relationships between basin-scale Sheltered Index (SI) and long-term fractional glacier loss. (a) Signed fractional area change versus glacier-median SI ($r = -0.609$, $p = 0.00059$, $n = 28$), and (b) signed fractional first-order estimated-volume change versus glacier-median SI ($r = -0.673$, $p = 8.7 \times 10^{-5}$, $n = 28$). Negative change values represent glacier loss, and higher SI values indicate greater terrain sheltering. Glacier change is calculated from 1947 to the 2025 mapped extent for Big Ben and from 1947 to the most recent mapped extent (2017) for the Laurens Peninsula. Lines show ordinary least-squares linear fits.

SI was therefore associated with a substantial but incomplete component of the spatial variation in long-term glacier loss, with approximately 37 % and 45 % of the glacier-to-glacier variance in fractional area and estimated-volume change, respectively, associated with SI in these linear relationships.

### 3.6 Glacier–climate associations

Contemporaneous seasonal glacier–climate correlations varied substantially among individual glaciers (Fig. 9). Correlations with both SST and wind-stress magnitude differed in magnitude and sign among glaciers and seasons, and no individual seasonal variable produced a consistent association across the glacier population.

https://doi.org/10.5194/egusphere-2026-6712
Preprint. Discussion started: 17 November 2026
© Author(s) 2026. CC BY 4.0 License.

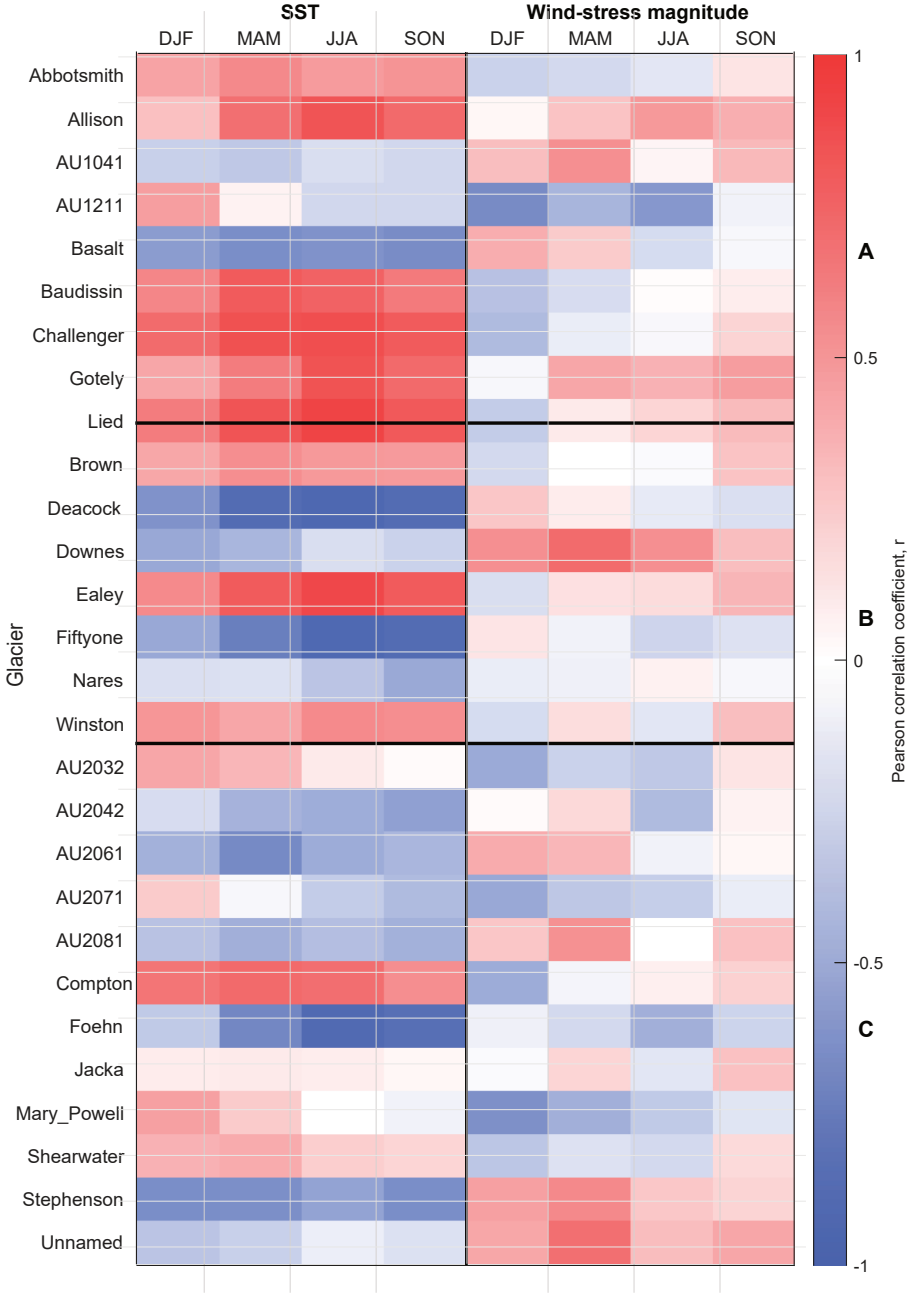



**Figure 9.** Contemporaneous Pearson correlations between five-year glacier-change trajectories and seasonal SST and wind-stress magnitude for the 28 Heard Island glaciers. Columns show correlations for DJF, MAM, JJA, and SON, and glaciers are arranged by final attribute-based response group (A–C). Horizontal lines separate the three groups. Colours show the Pearson correlation coefficient ($r$), ranging from negative (blue) to positive (red) associations. Response-group assignment does not include the climate correlations shown here.

https://doi.org/10.5194/egusphere-2026-6712
Preprint. Discussion started: 17 November 2026
© Author(s) 2026. CC BY 4.0 License.

The final attribute-based response groups showed substantial overlap in their climate associations. Median maximum absolute SST correlations were 0.798, 0.560, and 0.455 for Groups A, B, and C, respectively, while median maximum absolute wind-stress magnitude correlations were 0.394, 0.288, and 0.494. The ranges within each group were broad: maximum absolute SST correlations ranged from 0.317–0.924 in Group A, 0.508–0.913 in Group B, and 0.100–0.877 in Group C; corresponding wind-stress magnitude ranges were 0.261–0.653, 0.109–0.716, and 0.294–0.693.

These overlapping distributions did not identify discrete SST- or wind-stress-associated response regimes among Groups A–C. The correlations are therefore treated as descriptive contemporaneous associations rather than evidence that the response groups represent distinct modes of climatic forcing.

### 3.7 Attribute-based glacier-response groups

The attribute-based classification assigned nine glaciers to Group A, seven to Group B, and 12 to Group C (Table S1). All 28 glaciers received a unique highest score. Geographic region, longitude, and glacier–climate correlations were excluded from group assignment, allowing the spatial distribution and climate associations of the resulting groups to be evaluated independently.

The groups showed pronounced differences in terrain exposure and long-term glacier loss (Fig. 10). Group A had the lowest glacier-median SI (median 0.415; range 0.349–0.456) and generally the smallest long-term losses. Median area change was $-7.64\,\%$ (range $-49.37$ to $+0.27\,\%$), and median first-order estimated-volume change was $-9.38\,\%$ (range $-52.75$ to $-0.59\,\%$). Median elevation was 647 m (range 485–1236 m).

Group B occupied intermediate to sheltered terrain, with a median SI of 0.531 (range 0.459–0.615). Long-term losses were larger than in Group A, with median area and estimated-volume changes of $-28.75\,\%$ (range $-42.48$ to $-6.90\,\%$) and $-27.60\,\%$ (range $-47.63$ to $-4.74\,\%$), respectively. Median elevation was 669 m (range 508–891 m), indicating that elevation alone did not differentiate Groups A and B.

Group C had the highest median SI (0.572; range 0.488–0.649) and the largest long-term losses. Median area change was $-62.97\,\%$ (range $-97.87$ to $-43.25\,\%$), while median first-order estimated-volume change was $-70.41\,\%$ (range $-97.45$ to $-61.41\,\%$). Group C also had the lowest median elevation, at 531 m, although individual elevations ranged from 269 to 865 m. The groups therefore describe a progression from low-SI glaciers with generally small losses in Group A through an intermediate response in Group B to higher-SI glaciers with substantially larger losses in Group C.

https://doi.org/10.5194/egusphere-2026-6712
Preprint. Discussion started: 17 November 2026
© Author(s) 2026. CC BY 4.0 License.

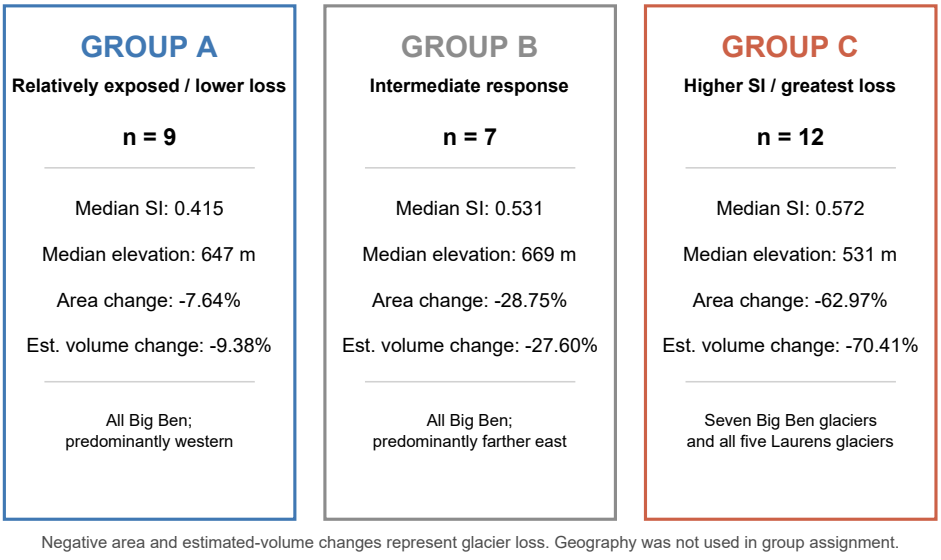



**Figure 10.** Summary characteristics of the three attribute-based glacier-response groups. Values are group medians for basin-scale Sheltered Index (SI), endpoint median elevation, fractional area change, and first-order estimated-volume change. Endpoint glacier geometry corresponds to 2025 for Big Ben and the most recent mapped extent in 2017 for the Laurens Peninsula. The groups summarise recurring combinations of terrain exposure, glacier elevation, and long-term loss rather than independently evaluated physical glacier types.

Despite geography being excluded from the classification, the groups showed clear spatial organisation (Fig. 11). Groups A and B were confined to Big Ben, whereas Group C included seven Big Ben glaciers and all five glaciers on the Laurens Peninsula. Group A was concentrated on western Big Ben, while Group B occurred predominantly among Big Ben glaciers farther east. The occurrence of seven Group-C glaciers on Big Ben, together with local departures from the predominant A–B spatial pattern, shows that the classification although spatially organised, is not a restatement of geographic region.

https://doi.org/10.5194/egusphere-2026-6712
Preprint. Discussion started: 17 November 2026
© Author(s) 2026. CC BY 4.0 License.

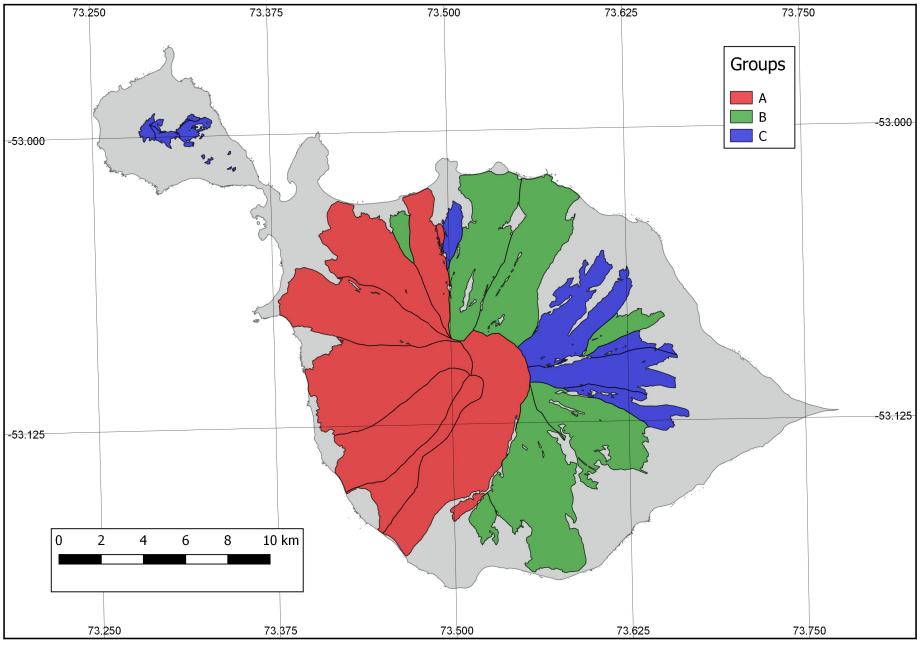



**Figure 11.** Spatial distribution of attribute-based glacier-response Groups A–C across Heard Island. Geographic region and longitude were excluded from the classification, which was based on glacier-median SI, median elevation, and long-term area and first-order estimated-volume change. The spatial organisation therefore emerged independently of geographic location.

The principal characteristics and predominant spatial settings of the three groups are summarised in Table 5.

https://doi.org/10.5194/egusphere-2026-6712
Preprint. Discussion started: 17 November 2026
© Author(s) 2026. CC BY 4.0 License.

**Table 5.** Summary characteristics of the final attribute-based glacier-response groups across Heard Island.

| Group | Predominant spatial setting | Terrain and elevation characteristics | Long-term glacier loss |
|---|---|---|---|
| A ($n = 9$) | Predominantly western Big Ben | Lowest SI (median 0.415; range 0.349–0.456); median elevation 647 m (485–1236 m) | Generally smallest losses; median area change $-7.64\,\%$ and estimated-volume change $-9.38\,\%$ |
| B ($n = 7$) | Big Ben; predominantly farther east than Group A | Intermediate to higher SI (median 0.531; range 0.459–0.615); median elevation 669 m (508–891 m) | Intermediate losses; median area change $-28.75\,\%$ and estimated-volume change $-27.60\,\%$ |
| C ($n = 12$) | Laurens Peninsula and seven Big Ben basins | Highest median SI (0.572; range 0.488–0.649); lowest median elevation, 531 m (269–865 m) | Largest losses; median area change $-62.97\,\%$ and estimated-volume change $-70.41\,\%$ |

## 4 Discussion

### 4.1 Regional climate variability and limits of climatic attribution

The glacier retreat observed on Heard Island since 1947 occurred within a region characterised by substantial multi-decadal oceanic and atmospheric variability (Rintoul, 2018; Bakke et al., 2021; Cai et al., 2023). The climate record analysed here shows positive SST trends in all seasons between 1965 and 2025, although only the JJA trend was statistically significant at the 0.05 level. Seasonal wind-stress magnitude also showed positive linear trends, but none was statistically significant. These results establish a regional climatic context for the observed glacier losses without showing that any individual climate variable was the direct cause of glacier retreat.

The glacier–climate correlations support this distinction. Contemporaneous correlations between five-year glacier-change trajectories and seasonal SST and wind-stress magnitude varied considerably among glaciers and seasons (Fig. 9). Both positive and negative correlations occurred within the glacier population, and no individual seasonal climate variable produced a consistent association across all glaciers. The final response groups also showed broad overlap in their climate-correlation distributions. The median maximum absolute SST correlations decreased from Group A to Groups B and C, whereas the maximum absolute wind-stress correlations did not show a corresponding monotonic progression. The groups therefore cannot be interpreted as discrete SST-, wind-stress-, or compound-forcing regimes.

Several aspects of the analysis limit stronger climatic attribution. The climate data represent a common regional time series rather than glacier-specific climatic conditions, while the five-year glacier trajectories contain interpolated values between a

https://doi.org/10.5194/egusphere-2026-6712
Preprint. Discussion started: 17 November 2026
© Author(s) 2026. CC BY 4.0 License.

limited number of independent glacier inventories. The correlations are contemporaneous and do not resolve temporal lags. In addition, SST and surface wind stress are regional environmental indicators rather than direct measurements of surface energy and mass-balance processes operating on individual glaciers. Therefore, observed correlations should be interpreted as descriptive associations within the regional climate system rather than quantitative estimates of climatic forcing (Roe, 2010).

This distinction is important for SST. Ocean temperature can provide information on the broader maritime climate surrounding Heard Island, but the present analysis does not establish a direct ocean-to-glacier mechanism (Cai et al., 2023; Zanker et al., 2024). Variability in SST may be co-correlated with atmospheric temperature, moisture transport, precipitation phase, cloud conditions, or other components of the regional climate system that influence glacier surface mass balance. Resolving these pathways would require glacier-scale meteorological and mass-balance observations that are not currently available. The SST record is therefore interpreted as part of the regional climatic context within which glacier retreat occurred.

### 4.2 Topographic exposure, glacier geometry, and spatial asymmetry

The pronounced spatial variability in glacier loss shows that a common regional climatic setting did not produce a uniform glacier response. Long-term fractional losses differed markedly between individual basins and among the principal geographic sectors of Heard Island. Western Big Ben glaciers had a median area change of $-10.77\,\%$, compared with $-42.39\,\%$ for eastern Big Ben and $-81.42\,\%$ for the Laurens Peninsula. Corresponding median first-order estimated-volume changes were $-12.50\,\%$, $-47.28\,\%$, and $-78.87\,\%$, respectively. The Big Ben changes extend to 2025, whereas the Laurens Peninsula changes extend to its most recent mapped glacier extent in 2017. These contrasts indicate substantial local modulation of glacier loss within the broader regional climate setting.

Terrain exposure provides one quantitative descriptor of this spatial variability. Glacier-median SI was significantly negatively correlated with both signed fractional area change ($r = -0.609$) and first-order estimated-volume change ($r = -0.673$). Because negative change values represent glacier loss, these relationships indicate that glaciers with higher SI values, that is, relatively more sheltered basins, generally experienced larger fractional losses. This result does not support a simple model in which greater exposure to the prevailing wind environment necessarily produces larger glacier loss. Rather, several of the largest fractional changes occurred among sheltered glaciers on eastern and southeastern Heard Island.

A plausible contribution to this spatial asymmetry is the development of precipitation-shadow and foehn effects in the lee of Big Ben under prevailing westerly airflow. Orographic precipitation on windward slopes could reduce snowfall reaching eastern and southeastern glaciers, while descending lee-side air may undergo warming and drying, potentially favouring surface ablation. Foehn-related warming and surface melting have been documented on the eastern Antarctic Peninsula (Elvidge et al., 2015; Kuipers Munneke et al., 2018). Such mechanisms could contribute to greater fractional losses in relatively sheltered basins despite their reduced direct exposure to prevailing winds. However, the present analysis does not resolve local precipitation gradients, foehn occurrence, or glacier-scale surface-energy balance and therefore cannot establish their contribution to the observed retreat. The eastern and southeastern Big Ben glaciers provide a setting in which these hypotheses could be tested using targeted meteorological observations and high-resolution atmospheric modelling.

https://doi.org/10.5194/egusphere-2026-6712
Preprint. Discussion started: 17 November 2026
© Author(s) 2026. CC BY 4.0 License.

Spatial statistics show the same pattern. Median SI increased from 0.447 for western Big Ben to 0.559 for eastern Big Ben and 0.592 for the Laurens Peninsula, while median fractional glacier loss also increased across these sectors. SI nevertheless accounted for only part of the variability between glaciers, because the $r^2$ values of approximately 0.37 for area change and 0.45 for estimated-volume change leave substantial variability unexplained. Terrain sheltering should therefore not be regarded as a direct predictor of glacier response. Rather, SI describes one component of the local topographic setting within which glacier loss occurred.

Glacier geometry provides an additional source of spatial differentiation, consistent with the importance of glacier morphology and elevation in modulating glacier response to climatic variability (Brun et al., 2019; Noël et al., 2020). Laurens Peninsula glaciers occupy substantially lower and narrower elevation ranges than many Big Ben glaciers and have a median elevation of 437 m, compared with 557 m for western Big Ben and 717 m for eastern Big Ben. They are also substantially steeper, with a median slope of $24^\circ$ compared with $14^\circ$ and $13^\circ$ for western and eastern Big Ben, respectively. At glacier scale, median slope was negatively correlated with signed fractional area change ($r = -0.568$, $p = 0.0016$), with steeper glaciers tending to show larger fractional loss. This association should not be interpreted as evidence that slope itself caused the observed retreat, because slope covaries with other aspects of glacier size, elevation range, and topographic setting.

The restricted high-elevation area of the Laurens Peninsula glaciers may also reduce the capacity of these glaciers to redistribute glacier area toward colder elevations as climatic conditions change (Cuffey and Paterson, 2010; Noël et al., 2020). In contrast, the broader hypsometric ranges of many Big Ben glaciers provide substantially larger high-elevation glacier area. This geometric contrast offers a plausible explanation for part of the strong difference in fractional loss between the two regions. However, equilibrium-line altitude (ELA) was not reconstructed in this study, and the degree to which individual glacier hypsometry controlled long-term retreat cannot be directly quantified. The observed patterns are therefore consistent with differences in hypsometric buffering rather than showing a specific elevation threshold or ELA-driven response.

### 4.3 Interpretation of attribute-based glacier-response groups

The attribute-based classification provides a compact representation of the continuum of glacier responses across Heard Island. Nine glaciers were assigned to Group A, seven to Group B, and 12 to Group C. The classification used glacier-median SI, median elevation, and long-term area and first-order estimated-volume change. Geographic location and glacier–climate correlations were deliberately excluded. The resulting groups should therefore be interpreted as comparative classes defined by measured and derived glacier attributes rather than as independently evaluated physical glacier types.

Group A contains low-SI glaciers and is characterised by generally small long-term fractional losses. Median area and estimated-volume changes in Group A were $-7.64\,\%$ and $-9.38\,\%$, respectively. Group B occupies intermediate to sheltered terrain and shows intermediate losses, with median area and estimated-volume changes of $-28.75\,\%$ and $-27.60\,\%$. Group C has the highest median SI and substantially greater losses, with median area and estimated-volume changes of $-62.97\,\%$ and $-70.41\,\%$, respectively. Group C also has the lowest median elevation (531 m), although the range extends to 865 m. Elevation therefore contributes to the distinction among response groups but does not alone determine group membership.

https://doi.org/10.5194/egusphere-2026-6712
Preprint. Discussion started: 17 November 2026
© Author(s) 2026. CC BY 4.0 License.

The classification also shows a spatial organisation that was not imposed by the scoring procedure. Groups A and B occur entirely on Big Ben, whereas Group C includes all five Laurens Peninsula glaciers together with seven Big Ben glaciers. Group A occurs predominantly on western Big Ben, while Group B is more common farther east. The occurrence of seven Group-C glaciers on Big Ben shows that the classification is not simply reproducing the geographic division between Big Ben and the Laurens Peninsula. Individual Big Ben basins can exhibit the high-loss attribute combination characteristic of Group C despite occupying the main volcanic massif.

The progression in long-term loss from Groups A through C occurs alongside an increase in median SI, but the geometric characteristics are less uniform. Median elevation is similar between Groups A and B (647 and 669 m, respectively) and substantially lower in Group C (531 m), while elevation ranges overlap among all three groups. The classification therefore captures combinations of terrain exposure, geometry, and observed response rather than a single controlling gradient. In particular, the presence of relatively high-elevation glaciers within Group C shows that elevation is not a necessary condition for large fractional loss.

The independent climate comparison provides a further test of the meaning of these groups. Climate correlations were not used in their assignment, and the resulting SST and wind-stress correlation distributions overlap substantially among Groups A–C. Consequently, the classification does not support labels such as “SST-sensitive”, “wind-sensitive”, or “compound-forcing” glacier types. Instead, Groups A–C provide an attribute-based framework for describing the spatial heterogeneity of glacier response and for identifying combinations of glacier characteristics associated with different magnitudes of long-term loss.

### 4.4 Southern Ocean context and broader implications

The widespread glacier losses documented here extend a history of glacier recession on Heard Island identified from earlier observations and glacier inventories (Allison and Keage, 1986; Thost and Truffer, 2008). The present results further show that this island-wide retreat has been spatially heterogeneous, with marked differences in fractional loss among individual glacier basins. Heard Island provides a useful setting for examining spatially variable glacier response because a small glacierised island contains strong contrasts in elevation, hypsometry, terrain exposure, and glacier size while remaining embedded within a broadly shared maritime climate. The observed pattern shows that substantial differences in long-term glacier loss can occur over short spatial distances even where glaciers experience the same regional-scale oceanic and atmospheric variability.

The results therefore favour a regional-climate–local-modulation framework rather than a simple single-forcing explanation (Fig. 12). Regional Southern Ocean and atmospheric variability provides the climatic context within which the glaciers evolve, while local terrain exposure, elevation, hypsometry, size, and topographic setting are associated with differences in the expression of glacier loss among individual basins. These local characteristics need not operate independently and may influence glacier response through several interacting processes.

For example, lower-elevation maritime glaciers may contain a larger proportion of their area under conditions favourable for surface melt or rain rather than snow during relatively warm periods (Noël et al., 2020; Cuffey and Paterson, 2010). Restricted high-elevation accumulation areas may further limit the capacity of small glaciers to maintain area at colder elevations. Terrain setting may influence snow redistribution, shading, and local surface-energy conditions (Dadić et al., 2010; Mott et al.,

https://doi.org/10.5194/egusphere-2026-6712
Preprint. Discussion started: 17 November 2026
© Author(s) 2026. CC BY 4.0 License.

2020; Shaw et al., 2024). Such processes provide physically plausible pathways by which regional climatic variability could produce heterogeneous glacier responses. They remain hypotheses in the present study, however, because surface mass balance, precipitation phase, snow redistribution, and glacier-scale meteorological conditions were not measured directly.

The Heard Island results also illustrate a broader methodological point for remote maritime and sub-Antarctic glacier systems. Regional climate indices alone may be insufficient to explain spatial patterns of glacier loss, particularly where neighbouring glaciers differ strongly in geometry and topographic setting (Roe, 2010; Brun et al., 2019). Conversely, correlations between glacier loss and terrain attributes should not be interpreted independently of the regional climate in which those glaciers are embedded. Combining multi-temporal glacier inventories with terrain metrics and regional climate records can therefore provide a useful framework for identifying spatial patterns and formulating process-based hypotheses, even where direct glaciological observations remain limited.

Several uncertainties constrain the interpretation of the present results. Glacier area is derived from a limited number of historical and satellite inventory epochs, while the five-year trajectories between these epochs are interpolated and do not represent independent observations. Persistent cloud cover prevented reliable remapping of the Laurens Peninsula after 2017, so its 2017 glacier outlines were retained in the nominal 2019 and 2025 inventory fields. Long-term changes for the Laurens Peninsula therefore terminate at the most recent mapped extent in 2017, whereas Big Ben has an updated observational endpoint in 2025. Glacier volume is a first-order estimate based on simplified thickness assumptions and glacier-specific area–volume scaling and should not be interpreted as a geodetic reconstruction of ice volume or mass balance (Bahr et al., 1997; Farinotti et al., 2009). In particular, the method does not independently measure surface-elevation changes or thinning within the remaining glacierised area. The resulting density-equivalent mass loss is therefore not directly comparable with geodetic mass balances derived from observed elevation changes, such as those reported for South Georgia and the Cook Ice Cap on Kerguelen (Farías-Barahona et al., 2020; Favier et al., 2016). Satellite-derived geodetic assessments also provide a distinct basis for estimating glacier mass changes over more recent periods (Hugonnet et al., 2021). Differences in methodology, observation period, and geographic setting preclude direct inference of a correction factor for the Heard Island estimates. Furthermore, SI represents a basin-scale terrain descriptor rather than a direct measure of climatic forcing, and the regional climate series does not resolve glacier-scale atmospheric variability. These limitations restrict quantitative attribution but do not alter the principal observational result: glacier loss across Heard Island has been spatially heterogeneous.

https://doi.org/10.5194/egusphere-2026-6712
Preprint. Discussion started: 17 November 2026
© Author(s) 2026. CC BY 4.0 License.

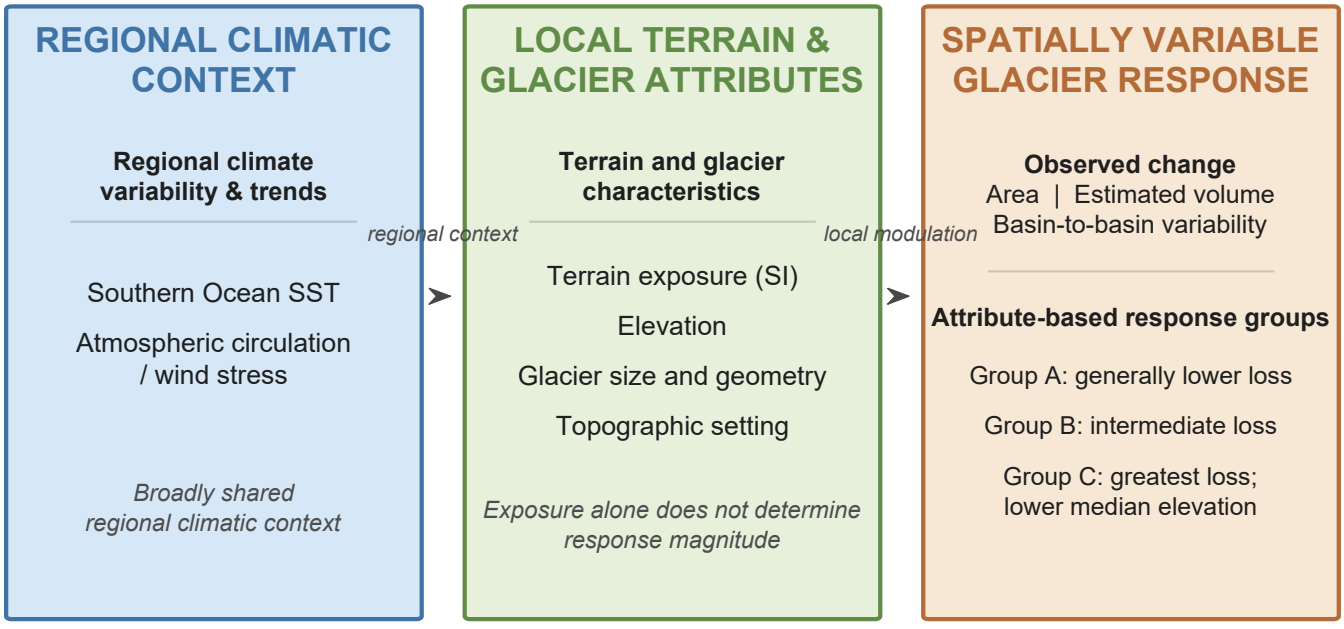



**Figure 12.** Conceptual regional-climate–local-modulation framework for spatially heterogeneous glacier change on Heard Island. Regional Southern Ocean and atmospheric variability provides a broadly shared climatic context, while glacier-specific terrain exposure, elevation, geometry, and topographic setting may modulate glacier response within this regional climatic context. The resulting spatially variable response is expressed through differences in glacier area and first-order estimated-volume change and summarised by the attribute-based response groups. Arrows represent hypothesised interactions rather than quantified causal pathways.

Taken together, the results show that Heard Island glacier loss cannot be described adequately by either regional climate variability or local terrain attributes in isolation. Regional climate variability provides a broadly shared climatic context within which local terrain and glacier characteristics are associated with spatially heterogeneous glacier loss. Spatially heterogeneous glacier response under a shared regional climate is consistent with the broader influence of glacier morphology and local topographic conditions on glacier response (Brun et al., 2019; Noël et al., 2020). This interpretation accounts for the coexistence of relatively stable and strongly retreating glaciers within the same regional climate setting while remaining consistent with the observational and methodological limits of the present analysis.

## 5 Conclusions

Glaciers on Heard Island underwent substantial and spatially heterogeneous retreat over the period examined, from 1947 to 2025 for Big Ben and from 1947 to 2017 for the Laurens Peninsula. Total glacierised area decreased from 283.73 to 217.96 $km^2$ (23.18 %), while first-order estimated ice volume decreased from 17.59 to 12.08 $km^3$ (31.33 %), equivalent to an estimated 4.96 Gt of ice under an assumed density of 900 $kg\,m^{-3}$. The nominal 2025 island-wide inventory combines the 2025 Big Ben

https://doi.org/10.5194/egusphere-2026-6712
Preprint. Discussion started: 17 November 2026
© Author(s) 2026. CC BY 4.0 License.

outlines with the latest reliably mapped Laurens Peninsula outlines from 2017. Losses were strongly spatially heterogeneous, demonstrating that glaciers within a broadly shared maritime climate setting did not undergo uniform retreat.

The spatial contrasts were pronounced. Western Big Ben glaciers had a median fractional area loss of 10.77 %, compared with 42.39 % for eastern Big Ben and 81.42 % for the Laurens Peninsula. Glacier-median Sheltered Index (SI) was significantly negatively correlated with signed fractional area change and first-order estimated-volume change, indicating that relatively more sheltered glaciers generally experienced greater fractional losses. An attribute-based classification distinguished three groups comprising 9, 7, and 12 glaciers, respectively, ranging from generally smaller losses in more exposed terrain to greater losses among relatively sheltered glaciers. Although geographic location was excluded from classification, the groups exhibited pronounced spatial organisation. Terrain exposure, elevation, hypsometry, and glacier geometry were therefore associated with the spatial expression of glacier loss, although these relationships do not establish individual causal mechanisms.

These findings support a regional-climate–local-modulation framework in which Southern Ocean and atmospheric variability provides a broadly shared climatic context, while local terrain and glacier characteristics are associated with contrasting glacier responses. Contemporaneous correlations with seasonal sea-surface temperature and wind-stress magnitude overlapped among the three groups and did not identify distinct physical response regimes. For Heard Island and other maritime Southern Ocean islands, multi-temporal glacier inventories combined with terrain analysis can help identify spatial patterns and formulate testable hypotheses where direct observations remain limited. Continued glacier mapping, geodetic measurements of ice-surface elevation change, and observations of accumulation, surface mass balance, and local meteorological conditions are needed to evaluate potential mechanisms, including precipitation-shadow and foehn effects, and to establish how these spatial contrasts evolve under future climate variability.

## code availability

The MATLAB scripts used to generate glacier metrics, sensitivity-group classifications, and figures are available from the corresponding author upon reasonable request.

## data availability

The glacier inventory outlines, glacier morphometric attributes, Sheltered Index (SI) data, and derived glacier area and estimated-volume change tables used in this study are publicly available through the Australian Antarctic Data Centre (AADC) at xxxxxxxxxxxxx. The deposited dataset includes the available observational inventory epochs and identifies the 2017 Laurens Peninsula outlines carried forward into the nominal 2019 and 2025 inventory fields. The ORAS5 ocean reanalysis data used to derive regional sea-surface temperature and surface wind-stress indicators are available from the European Centre for Medium-Range Weather Forecasts (ECMWF).

https://doi.org/10.5194/egusphere-2026-6712
Preprint. Discussion started: 17 November 2026
© Author(s) 2026. CC BY 4.0 License.

**authorcontribution**

RPS designed the methodology, compilation of data and analysis with contributions from all co-authors. SD compiled and edited much of the glacial inventory. BGF provided guidance on the regional oceanographic and climatic process and general guidance as the study developed. RPS prepared the manuscript with contributions from all co-authors.

**competing interests**

The authors declare that they have no conflict of interest.

**acknowledgements**

The authors thank two reviewers for their highly constructive and insightful comments on an earlier version of this manuscript. This work is supported by the Australian Antarctic Division, the Antarctic Partnership Program (AAPP) funded by the Australian Government Department of Industry, Science, Energy and Resources through the Antarctic Science Collaboration Initiative.

https://doi.org/10.5194/egusphere-2026-6712
Preprint. Discussion started: 17 November 2026
© Author(s) 2026. CC BY 4.0 License.

## References

Allison, I. and Keage, P.: Recent changes in the glaciers of Heard Island, Polar Record, 23, 255–272, https://doi.org/10.1017/s0032247400007099, 1986.

Bahr, D. B., Meier, M. F., and Peckham, S. D.: The physical basis of glacier volume-area scaling, Journal of Geophysical Research: Solid Earth, 102, 20 355–20 362, https://doi.org/10.1029/97JB01696, 1997.

Bakke, J., Paasche, Ø., Schaefer, J., and Timmermann, A.: Long-term demise of sub-Antarctic glaciers modulated by the Southern Hemisphere Westerlies, Scientific Reports, 11, https://doi.org/10.1038/s41598-021-87317-5, 2021.

Brun, F., Wagnon, P., Berthier, E., Jomelli, V., Maharjan, S., Shrestha, F., and Kraaijenbrink, P.: Heterogeneous Influence of Glacier Morphology on the Mass Balance Variability in High Mountain Asia, Journal of Geophysical Research: Earth Surface, 124, 1331 – 1345, https://doi.org/10.1029/2018jf004838, 2019.

Cai, W., Gao, L., Luo, Y., Li, X., Zheng, X., Zhang, X., Cheng, X., Jia, F., Purich, A., Santoso, A., Du, Y., Holland, D., Shi, J., Xiang, B., and Xie, S.: Southern Ocean warming and its climatic impacts., Science bulletin, https://doi.org/10.1016/j.scib.2023.03.049, 2023.

Chassiot, L., Chapron, E., Michel, E., Jomelli, V., Favier, V., Verfaillie, D., Foucher, A., Charton, J., Paterne, M., and der Putten, N. V.: Late Holocene record of subantarctic glacier variability in Table Fjord, Cook Ice Cap, Kerguelen Islands, Quaternary Science Reviews, https://doi.org/10.1016/j.quascirev.2024.108980, 2024.

Clem, K., Bozkurt, D., Kennett, D., King, J., and Turner, J.: Central tropical Pacific convection drives extreme high temperatures and surface melt on the Larsen C Ice Shelf, Antarctic Peninsula, Nature Communications, 13, https://doi.org/10.1038/s41467-022-31119-4, 2022.

Cuffey, K. M. and Paterson, W. S. B.: The physics of glaciers, Academic Press, 2010.

Dadić, R., Mott, R., Lehning, M., and Burlando, P.: Wind influence on snow depth distribution and accumulation over glaciers, Journal of Geophysical Research, 115, https://doi.org/10.1029/2009jf001261, 2010.

Deng, K., Azorín-Molina, C., Yang, S., Hu, C., Zhang, G., Minola, L., and Chen, D.: Changes of Southern Hemisphere westerlies in the future warming climate, Atmospheric Research, https://doi.org/10.1016/j.atmosres.2022.106040, 2022.

Desbiolles, F., Blamey, R., Illig, S., James, R., Barimalala, R., Renault, L., and Reason, C.: Upscaling impact of wind/sea surface temperature mesoscale interactions on southern Africa austral summer climate, International Journal of Climatology, 38, 4651 – 4660, https://doi.org/10.1002/joc.5726, 2018.

Donoghue, S.: Changes in the morphology, mass balance, and dynamics of Brown Glacier, Heard Island, with comparison to the surrounding sub-Antarctic islands, PhD dissertation, University of Tasmania, Hobart, Tasmania, 2009.

Elvidge, A. D., Renfrew, I. A., King, J. C., Orr, A., Lachlan-Cope, T. A., Weeks, M., and Gray, S. L.: Foehn jets over the Larsen C ice shelf, Antarctica, Quarterly Journal of the Royal Meteorological Society, 141, 698–713, https://doi.org/10.1002/qj.2382, 2015.

Evans, I.: World-Wide Variations in the Direction and Concentration of Cirque and Glacier Aspects, Geografiska Annaler Series A-physical Geography, 59, 151–175, https://doi.org/10.1080/04353676.1977.11879949, 1977.

Farías-Barahona, D., Sommer, C., Sauter, T., Bannister, D., Seehaus, T. C., Malz, P., Casassa, G., Mayewski, P. A., Turton, J. V., and Braun, M. H.: Detailed quantification of glacier elevation and mass changes in South Georgia, Environmental Research Letters, 15, 034 036, https://doi.org/10.1088/1748-9326/ab6b32, 2020.

Farinotti, D., Huss, M., Bauder, A., Funk, M., and Truffer, M.: A method to estimate the ice volume and ice-thickness distribution of alpine glaciers, Journal of Glaciology, 55, 422–430, https://doi.org/10.3189/002214309788816759, 2009.

https://doi.org/10.5194/egusphere-2026-6712
Preprint. Discussion started: 17 November 2026
© Author(s) 2026. CC BY 4.0 License.

Favier, V., Verfaillie, D., Berthier, E., Menegoz, M., Jomelli, V., Kay, J. E., Ducret, L., Malbéteau, Y., Brunstein, D., Gallée, H., Park, Y. H., and Rinterknecht, V.: Atmospheric drying as the main driver of dramatic glacier wastage in the southern Indian Ocean, Scientific Reports, 6, 32 396, https://doi.org/10.1038/srep32396, 2016.

Fritsch, F. N. and Carlson, R. E.: Monotone piecewise cubic interpolation, SIAM Journal on Numerical Analysis, 17, 238–246, https://doi.org/10.1137/0717021, 1980.

Gorodetskaya, I., Durán-Alarcón, C., González-Herrero, S., Clem, K., Zou, X., Rowe, P., Imazio, P. R., Campos, D., Santos, L.-D., Dutrievoz, N., Wille, J., Chyhareva, A., Favier, V., Blanchet, J., Pohl, B., Cordero, R., Park, S., Colwell, S., Lazzara, M., Carrasco, J., Gulisano, A., Krakovska, S., Ralph, F., Dethinne, T., and Picard, G.: Record-high Antarctic Peninsula temperatures and surface melt in February 2022: a compound event with an intense atmospheric river, npj Climate and Atmospheric Science, 6, 1–18, https://doi.org/10.1038/s41612-023-00529-6, 2023.

Holland, D., Nicholls, K., and Basinski, A.: The Southern Ocean and its interaction with the Antarctic Ice Sheet, Science, 367, 1326 – 1330, https://doi.org/10.1126/science.aaz5491, 2020.

Holland, P.: Ocean forcing of glacier retreat in the western Antarctic Peninsula, Science, 353, 283 – 286, https://doi.org/10.1126/science.aae0017, 2016.

Hugonnet, R., McNabb, R., Berthier, E., Menounos, B., Nuth, C., Girod, L., Farinotti, D., Huss, M., Dussaillant, I., Brun, F., and Kääb, A.: Accelerated global glacier mass loss in the early twenty-first century, Nature, 592, 726–731, https://doi.org/10.1038/s41586-021-03436-z, 2021.

Kiernan, K. and McConnell, A.: Geomorphology of the Sub-Antarctic Australian Territory of Heard Island-McDonald Island, Australian Geographer, 30, 159–195, https://doi.org/10.1080/00049189993693, 1999.

King, J. C. and Turner, J.: Antarctic Meteorology and Climatology, Cambridge Atmospheric and Space Science Series, Cambridge University Press, Cambridge, UK, 1997.

Kuipers Munneke, P., Luckman, A. J., Bevan, S. L., Smeets, C. J. P. P., Gilbert, E., van den Broeke, M. R., Wang, W., Zender, C., Hubbard, B., and Ashmore, D.: Intense winter surface melt on an Antarctic ice shelf, Geophysical Research Letters, 45, 7615–7623, https://doi.org/10.1029/2018GL077899, 2018.

Marshall, G. J.: Trends in the Southern Annular Mode from observations and reanalyses, Journal of climate, 16, 4134–4143, https://doi.org/10.1175/1520-0442(2003)016<4134:TITSAM>2.0.CO;2, 2003.

McCune, B. and Keon, D.: Equations for potential annual direct incident radiation and heat load, Journal of vegetation science, 13, 603–606, https://doi.org/10.1111/j.1654-1103.2002.tb02087.x, 2002.

Mernild, S., Beckerman, A., Yde, J., Hanna, E., Malmros, J., Wilson, R., and Zemp, M.: Mass loss and imbalance of glaciers along the Andes Cordillera to the sub-Antarctic islands, Global and Planetary Change, 133, 109–119, https://doi.org/10.1016/j.gloplacha.2015.08.009, 2015.

Mott, R., Stiperski, I., and Nicholson, L.: Spatio-temporal flow variations driving heat exchange processes at a mountain glacier, The Cryosphere, https://doi.org/10.5194/tc-14-4699-2020, 2020.

Nicholson, L. and Stiperski, I.: Comparison of turbulent structures and energy fluxes over exposed and debris-covered glacier ice, Journal of Glaciology, 66, 543 – 555, https://doi.org/10.1017/jog.2020.23, 2020.

Noël, B., Jakobs, C. L., van Pelt, W. V., Lhermitte, S., Wouters, B., Kohler, J., Hagen, J., Luks, B., Reijmer, C., van de Berg, W. J., and van den Broeke, M. R.: Low elevation of Svalbard glaciers drives high mass loss variability, Nature Communications, 11, https://doi.org/10.1038/s41467-020-18356-1, 2020.

https://doi.org/10.5194/egusphere-2026-6712
Preprint. Discussion started: 17 November 2026
© Author(s) 2026. CC BY 4.0 License.

Oerlemans, J.: Glaciers and climate change, CRC Press, 2001.

Perren, B. B., Hodgson, D., Roberts, S., Sime, L., Nieuwenhuyze, W. V., Verleyen, E., and Vyverman, W.: Southward migration of the Southern Hemisphere westerly winds corresponds with warming climate over centennial timescales, Communications Earth & Environment, 1, https://doi.org/10.1038/s43247-020-00059-6, 2020.

Rintoul, S. R.: The global influence of localized dynamics in the Southern Ocean, Nature, 558, 209–218, https://doi.org/10.1038/s41586-018-0182-3, 2018.

Roe, G.: What do glaciers tell us about climate variability and climate change?, Journal of Glaciology, 57, 567 – 578, https://doi.org/10.3189/002214311796905640, 2010.

Rudolph, E. M., Hedding, D., Hodgson, D. A., Fabel, D., Gheorghiu, D., Shanks, R., and Nel, W.: A glacial chronology for sub-Antarctic Marion Island from MIS 2 and MIS 3, Quaternary Science Reviews, https://doi.org/10.1016/j.quascirev.2023.108485, 2024.

Ryan, B. C.: A mathematical model for diagnosis and prediction of surface winds in mountainous terrain, Journal of Applied Meteorology and Climatology, 16, 571–584, https://doi.org/10.1175/1520-0450(1977)016<0571:AMMFDA>2.0.CO;2, 1977.

Sallée, J.-B., Pellichero, V., Akhoudas, C., Pauthenet, E., Vignes, L., Schmidtko, S., Garabato, A. N., Sutherland, P., and Kuusela, M.: Summertime increases in upper-ocean stratification and mixed-layer depth, Nature, 591, 592–598, https://doi.org/10.1038/s41586-021-03303-x, 2021.

Shaw, T., Miyawaki, O., and Donohoe, A.: Stormier Southern Hemisphere induced by topography and ocean circulation, Proceedings of the National Academy of Sciences of the United States of America, 119, https://doi.org/10.1073/pnas.2123512119, 2022.

Shaw, T., Buri, P., McCarthy, M., Miles, E., and Pellicciotti, F.: Local Controls on Near Surface Glacier Cooling Under Warm Atmospheric Conditions, Journal of Geophysical Research: Atmospheres, 129, https://doi.org/10.1029/2023jd040214, 2024.

Thompson, D. W., Solomon, S., Kushner, P. J., England, M. H., Grise, K. M., and Karoly, D. J.: Signatures of the Antarctic ozone hole in Southern Hemisphere surface climate change, Nature geoscience, 4, 741–749, https://doi.org/10.1038/ngeo1296, 2011.

Thost, D. and Truffer, M.: Glacier Recession on Heard Island, Southern Indian Ocean, Arctic, Antarctic, and Alpine Research, 40, 199–214, https://doi.org/10.1657/1523-0430(06-084)[thost]2.0.co;2, 2008.

Tielidze, L. G., Mackintosh, A. N., and Yang, W.: Glacier inventories reveal an acceleration of Heard Island glacier loss over recent decades, The Cryosphere, 19, 2677–2694, https://doi.org/10.5194/tc-19-2677-2025, 2025.

Wei, Y. and Chen, D.: Impact of Antarctic topography and zonal variations in atmospheric forcing on high-latitude zonal variations in SST, Journal of Physical Oceanography, https://doi.org/10.1175/jpo-d-24-0174.1, 2025.

Zanker, J. C., Young, E. F., Holland, P., Haigh, I., and Brickle, P.: Oceanographic Variability in Cumberland Bay, South Georgia, and Its Implications for Glacier Retreat, Journal of Geophysical Research: Oceans, https://doi.org/10.1029/2023jc020507, 2024.